## PAPER

# Structure and reactivity of [Ru$^{II}$(terpy)(N^N)Cl]Cl complexes: consequences for biological applications†

Marta Chrzanowska,[a] Anna Katafias, ID *[a] Olga Impert, ID [a] Anna Kozakiewicz, ID [a] Andrzej Surdykowski,[a] Paulina Brzozowska,[a] Alicja Franke,[b] Achim Zahl,[b] Ralph Puchta ID [b,c] and Rudi van Eldik ID *[a,b,d]

The crystal structures of [Ru$^{II}$(terpy)(bipy)Cl]Cl·2H$_2$O and [Ru$^{II}$(terpy)(en)Cl]Cl·3H$_2$O, where terpy = 2,2′:6′,2″-terpyridine, bipy = 2,2′-bipyridine and en = ethylenediamine, were determined and compared to the structure of the complexes in solution obtained by multi-nuclear NMR spectroscopy in DMSO$_{d-6}$ as a solvent. In aqueous solution, both chlorido complexes aquate fully to the corresponding aqua complexes, *viz.* [Ru$^{II}$(terpy)(bipy)(H$_2$O)]$^{2+}$ and [Ru$^{II}$(terpy)(en)(H$_2$O)]$^{2+}$, within *ca.* 2 h and *ca.* 2 min at 37 °C, respectively. The spontaneous aquation reactions can only be suppressed by chloride concentrations as high as 2 to 4 M, *i.e.* concentrations much higher than that found in human blood. The corresponding aqua complexes are characterized by p$K_a$ values of *ca.* 10 and 11, respectively, which suggest a more labile coordinated water molecule in the case of the [Ru$^{II}$(terpy)(en)(H$_2$O)]$^{2+}$ complex. Substitution reactions of the aqua complexes with chloride, cyanide and thiourea show that the [Ru$^{II}$(terpy)(en)(H$_2$O)]$^{2+}$ complex is 30–60 times more labile than the [Ru$^{II}$(terpy)(bipy)(H$_2$O)]$^{2+}$ complex at 25 °C. Water exchange reactions for both complexes were studied by $^{17}$O-NMR and DFT calculations (B3LYP(CPCM)/def2tzvp// B3LYP/def2svp and ωB97XD(CPCM)/def2tzvp//B3LYP/def2svp). Thermal and pressure activation parameters for the water exchange and ligand substitution reactions support the operation of an associative interchange ($I_a$) process. The difference in reactivity between these complexes can be accounted for in terms of π-back bonding effects of the terpy and bipy ligands and steric hindrance on the bipy complex. Consequences for eventual biological application of the chlorido complexes are discussed.

[a]*Faculty of Chemistry, N. Copernicus University, Gagarina 7, 87-100 Toruń, Poland. E-mail: rudi.vaneldik@fau.de*
[b]*Department of Chemistry and Pharmacy, University of Erlangen-Nuremberg, Egerlandstr. 1, 91058 Erlangen, Germany*
[c]*Computer Chemistry Center, Department of Chemistry and Pharmacy, University of Erlangen-Nuremberg, Nägelsbachstr. 25, 91052 Erlangen, Germany*
[d]*Faculty of Chemistry, Jagiellonian University, Ingardena 3, 30-060 Krakow, Poland*
†Electronic supplementary information (ESI) available: Detailed structural information on the [Ru$^{II}$(terpy)(N^N)Cl]$^+$ complexes in solution from $^1$H-, $^{13}$C- and $^{15}$N-NMR studies; rate and activation parameters for the reaction of [Ru(terpy)(bipy)(H$_2$O)]$^{2+}$ with chloride and thiourea; rate and activation parameters for the reaction of [Ru(terpy)(en)(H$_2$O)]$^{2+}$ with thiourea and cyanide; a summary of DFT calculations; additional kinetic plots. CCDC 1480087 and 1508410. For ESI and crystallographic data in CIF or other electronic format see DOI: 10.1039/c7dt01669g

## Introduction

[Ru$^{II}$(terpy)(bipy)Cl]Cl (terpy = 2,2′:6′,2″-terpyridine and bipy = 2,2′-bipyridine) and their closely related complexes have been known for many years and received significant attention from several research groups working on different areas.[1–7] More recent studies have focused on their aqueous chemistry, sub-stitution behavior, possible role as anti-tumor reagents,[2–6] and catalytic role in water oxidation reactions.[7] Preliminary studies in our laboratories, however, showed that the chemistry involved in such reactions is not that straightforward as one would expect and we ran into difficulties in reproducing the published data.[2–6] We, therefore, performed detailed structural, spectroscopic and kinetic studies on the [Ru$^{II}$(terpy)(bipy)Cl]Cl complex and extended the work to the corresponding [Ru$^{II}$(terpy)(en)Cl]Cl (en = ethylenediamine) complex. We report the first crystal structure determinations for both complexes, as well as detailed NMR studies on their solution structures. Although the bipy complex has been known for over 50 years,[1] its crystal structure has not been reported before, presumably due to difficulties encountered with the location of the chloride counter ion in the presence of several waters of crystallization. Efforts from our side to grow suitable crystals were unsuccessful for this particular reason.

We are interested in these complexes because of their potential biological application in terms of anti-tumor activity,[3–6] their potential role in the redox biology of cells,[8] and the ability of bipy and terpy chelates to affect the lability of metal centers through σ donor and π back-bonding effects.

Such effects can, in principle, significantly affect the electrophilicity of the metal center and in turn the substitution behavior of such Ru(II) complexes.[9–12] Since it is well known that Ru(II) complexes are, in general, orders of magnitude more labile than the corresponding Ru(III) complexes,[13,14] the introduction of labilizing chelates may further affect the lability of such complexes, which should show up in the spontaneous aquation of $[Ru^{II}(terpy)(N^N)Cl]^+$ complexes. Interestingly, we found that both $[Ru^{II}(terpy)(bipy)Cl]^+$ and $[Ru^{II}(terpy)(en)Cl]^+$ aquate rather rapidly, and high chloride concentrations between 2 and 4 M are required to suppress their spontaneous aquation reactions. In addition, substitution reactions of the corresponding aqua complexes with chloride and thiourea showed practically the same kinetic data and activation parameters. These reactions, however, were much faster for $[Ru^{II}(terpy)(en)H_2O]^{2+}$ than those for $[Ru^{II}(terpy)(bipy)H_2O]^{2+}$. ^{17}O NMR was employed to study the mechanism of the water exchange reaction on both complexes. Temperature and pressure activation parameters for the studied water exchange and ligand substitution reactions suggest the operation of an associative interchange ($I_a$) substitution mechanism for both complexes. The mechanistic assignment for the water exchange reactions is supported by DFT calculations.

# Experimental

## Chemicals

All chemicals were of analytical reagent grade and used without further purification. $RuCl_3 \cdot xH_2O$, 2,2′:6′,2″-terpyridine, ethylenediamine, and 2,2′-bipyridine were purchased from Sigma-Aldrich and other reagents and solvents were from Avantor Performance Materials Poland SA. Doubly deionized water was used throughout all experiments.

## Synthesis of the complexes

The precursor $[Ru^{III}(terpy)Cl_3]$ was synthesized according to a literature procedure.[15] The $[Ru^{II}(terpy)(N^N)Cl]Cl$ complexes (N^N = en or bipy) were prepared by following a slightly modified published procedure.[2,5] $[Ru^{III}(terpy)Cl_3]$ (500 mg, 1.2 mmol), 2,2′-bipyridine (187 mg, 1.2 mmol) or ethylenediamine (0.10 ml, 1.5 mmol), lithium chloride (500 mg, ~11.8 mmol) and 0.50 ml of triethylamine in 110 ml of a deaerated ethanol/water (3 : 1) solution were heated under reflux for 3 h under an argon atmosphere. The synthetic solution was filtered while hot to remove any unreacted reagent. The filtrate was reduced to 1/3 with a rotary evaporator and cooled in a refrigerator for 48 h. Small brown metallic or purple crystals of $[Ru^{II}(terpy)(bipy)Cl]Cl$ or $[Ru^{II}(terpy)(en)Cl]Cl$, respectively, were collected on a frit and air-dried. Yield: $[Ru^{II}(terpy)(bipy)Cl]Cl$ – 310 mg (79%, the literature 64%), $[Ru^{II}(terpy)(en)Cl]$ – 433 mg (65%, the literature 44%). In the case of $[Ru^{II}(terpy)(bipy)Cl]Cl$ it turned out not to be easy to obtain suitable crystals for structure determination since in a number of cases the chloride counter ion was hidden by too many water molecules. Crystals of $[Ru^{II}(terpy)(bipy)Cl]Cl$ suitable for X-ray studies were obtained from an anhydrous ethanol solution.

## Instrumentation

UV-Vis spectral analyses and slow kinetic measurements were carried out on HP 8453 diode-array and Shimadzu UV-1601 PC spectrophotometers thermostated with an HP 89090 Peltier Temperature Controller and a Julabo F25 cryostat, respectively. Experiments at elevated pressure (5–150 MPa) were performed on a laboratory-made high-pressure stopped-flow instrument.[16]

ESI-MS spectra were recorded using a Bruker MicrOTOF-Q II instrument with 4.5 kV capillary voltage and a dry gas flow ($N_2$) of 4 l min$^{-1}$. Samples of the $[Ru(terpy)(N^N)Cl]Cl$ complexes dissolved in ultrapure water one day before the measurement were injected into an ESI-MS-TOF chamber calibrated according to the manufacturer's procedure (clusters of 10 mM sodium formate in an isopropanol : water mixture (1 : 1, v/v)). The flow rate was set at 3 μl min$^{-1}$. The MS measurements were performed in the positive ion mode and the selected range was from 50 to 3000 $m/z$.

NMR spectra were recorded on Bruker Avance-400 and Bruker Avance-700 NMR spectrometers in $DMSO_{d-6}$ solution. [1]H and ^{13}C chemical shifts were referenced to TMS, and ^{15}N chemical shifts were referenced to $CH_3NO_2$. ^{17}O NMR spectra were recorded on a Bruker Avance DRX 400WB spectrometer equipped with a spectrospin superconducting wide-bore magnet operating at a resonance frequency of 54.24 MHz at a magnetic induction of 9.4 T. The measurements at atmospheric pressure were performed with a commercial 5 mm Bruker broadband probe thermostated with a Bruker B-VT 3000 variable temperature unit. Relaxation rates were measured for water bound to diamagnetic centers of the Ru(II) complexes. The line widths at half-height of the signal were determined by a deconvolution procedure on the real part of the Fourier transformed spectra with a Lorentzian shape function in the data analysis module of Bruker Topspin 1.3 software. The temperature was adjusted with circulating, thermostated water (Colora thermostat WK 16) to ±0.1 °C of the desired value and monitored before each measurement with an internal Pt-resistance thermometer with an accuracy of ±0.2 °C. Enriched [17]O-labeled water (D-Chem Ltd, Tel Aviv, Israel) was used for the ^{17}O NMR water exchange experiments. Samples were prepared by dissolving solid $[Ru^{II}(terpy)(N^N)Cl]Cl$ complexes in water containing 0.1 M $MnSO_4$ to obtain a 0.03 M complex solution. After the addition of [17]O-labeled water (30% v/v of 10% enriched [17]$OH_2$), the complex solutions were kept at 25 °C for the spontaneous aquation reactions to occur over a period of ca. 10 h and ca. 20 min for the bipy and en complexes, respectively, before they were transferred to a NMR tube.

The pH of the solutions was measured with an Elmetron CP-505 pH meter. Values of the observed rate constant are presented as the average of 3–5 kinetic runs and were reproducible within ±2%.

## Crystal structures of [Ru$^{II}$(terpy)(bipy)Cl]Cl·2H$_2$O and [Ru$^{II}$(terpy)(en)Cl]Cl·3H$_2$O

The brown plate crystals of [Ru$^{II}$(terpy)(bipy)Cl]Cl·2H$_2$O were obtained from anhydrous ethanol, while the purple plate crystals of [Ru$^{II}$(terpy)(en)Cl]Cl·3H$_2$O were obtained from aqueous solution. The X-ray data were collected at 25.0 °C with an Oxford Sapphire CCD diffractometer using MoKα radiation ($\lambda$ = 0.71073 Å) and the $\omega$–2$\theta$ method. The analytical absorption correction was applied with the maximum and minimum transmissions of 0.9642 and 0.6893 (bipy complex) or 0.9246 and 0.8654 (en complex), respectively.[17] The structures were solved by direct methods and refined by the full-matrix least-squares method on $F^2$ using the SHELX-97 program package.[18] The hydrogen atoms have been located from the difference electron density maps and constrained during refinement.

### Quantum chemical methods

The GAUSSIAN09 suite of programs was used.[19] Density functional calculations were performed using the hybrid functional B3LYP,[20] in combination with the effective core potential def2svp.[21] All structures were characterized as local minima or true transition states by computation of vibrational frequencies. To further evaluate the relative energies, B3LYP/def2tzvp[21] and ωB97XD[22]/def2tzvp calculations were performed on the B3LYP/def2svp structures. The influence of the bulk solvent was probed using the CPCM model[23] for B3LYP/def2tzvp and ωB97XD/def2tzvp, denoted B3LYP(CPCM)/ def2tzvp and ωB97XD(CPCM)/def2tzvp. All energies are ZPE-corrected (B3LYP/def2svp).

# Results and discussion

## Structures of [Ru$^{II}$(terpy)(bipy)Cl]Cl·2H$_2$O and [Ru$^{II}$(terpy)(en)Cl]Cl·3H$_2$O

Suitable crystals of both complexes for X-ray analysis were obtained as described in the Experimental section. In the case of the bipy complex it was essential to avoid water during the crystal growth, since in a few cases the counter chloride ion could not be located in the crystal structure as a result of too many water molecules that scavenged the chloride anion. We assume that this may be the reason why the crystal structure of this well-known complex has not been reported before.

The data collection and refinement processes are summarized in Table 1, and selected bond lengths and angles are presented in Table 2. The asymmetric part of [Ru$^{II}$(terpy)(bipy)Cl]Cl·2H$_2$O consists of two [Ru$^{II}$(terpy)(bipy)Cl]$^+$ cations, two Cl$^-$ ions and four water molecules (see Fig. 1), while the asymmetric part of [Ru$^{II}$(terpy)(en)Cl]Cl·3H$_2$O consists of the [Ru$^{II}$(terpy)(bipy)Cl]$^+$ cation, Cl$^-$ ions and three water molecules (Fig. 2). The electron density map of [Ru$^{II}$(terpy)(en)Cl]Cl·3H$_2$O showed five sites for water molecules, for which the occupancy of four sites was set at 0.5 based on the density data. Ru1 and Ru2 ions in [Ru$^{II}$(terpy)(bipy)Cl]Cl·2H$_2$O are six-coordinate in the deformed octahedral geometry with one chloride ion, two N atoms of bipy

**Table 1** Crystal data and structure refinement parameters for [Ru$^{II}$(terpy)(bipy)Cl]Cl·2H$_2$O and [Ru$^{II}$(terpy)(en)Cl]Cl·3H$_2$O

| Identification code | [Ru$^{II}$(terpy)(bipy)Cl]Cl·2H$_2$O | [Ru$^{II}$(terpy)(en)Cl]Cl·3H$_2$O |
|---|---|---|
| CCDC | 1480087 | 1508410 |
| Empirical formula | C$_{25}$H$_{23}$Cl$_2$N$_5$O$_2$Ru | C$_{17}$H$_{25}$Cl$_2$N$_5$O$_3$Ru |
| Formula weight, g mol$^{-1}$ | 597.45 | 519.39 |
| Wavelength, Å | 0.71073 | 0.71073 |
| $T$, K | 293(2) | 293(2) |
| Crystal size, mm | 0.47 × 0.22 × 0.04 | 0.16 × 0.14 × 0.09 |
| Crystal shape, color | Plate, brown | Plate, purple |
| Crystal system | Triclinic | Triclinic |
| Space group | P$\bar{1}$ | P$\bar{1}$ |
| $a$, Å | 13.585(3) | 6.9580(10) |
| $b$, Å | 13.764(3) | 13.352(3) |
| $c$, Å | 14.616(3) | 13.490(3) |
| $\alpha$, ° | 100.75(3) | 101.48(3) |
| $\beta$, ° | 101.21(3) | 92.81(3) |
| $\gamma$, ° | 100.51(3) | 103.84(3) |
| Volume, Å$^3$ | 2565.1(10) | 1186.4(4) |
| $Z$ | 4 | 2 |
| Density (calc.), g cm$^{-3}$ | 1.547 | 1.454 |
| Absorption coefficient, mm$^{-1}$ | 0.852 | 0.911 |
| $F$(000) | 1208 | 528 |
| $\Theta$ range, ° | 2.36 to 23.25 | 2.46 to 23.25 |
| Reflections collected/unique | 12 577/7319 [$R$(int) = 0.0685] | 6173/3394 [$R$(int) = 0.0657] |
| Index ranges $hkl$ | −12 ≤ h ≤ 15, −15 ≤ k ≤ 15, −16 ≤ l ≤ 16 | −7 ≤ h ≤ 7, −14 ≤ k ≤ 14, −14 ≤ l ≤ 14 |
| Restraints/parameters | 24/632 | 20/271 |
| Goodness of fit on $F^2$ | 1.090 | 1.091 |
| Final $R$ indices [$I > 2\sigma(I)$] | $R_1$ = 0.0789, w$R_2$ = 0.1657 | $R_1$ = 0.0832, w$R_2$ = 0.2392 |
| $R$ indices (all data) | $R_1$ = 0.1481, w$R_2$ = 0.2071 | $R_1$ = 0.1115, w$R_2$ = 0.2602 |
| Max electron density/e Å$^{-3}$ | 1.006 | 1.491 |
| Min electron density/e Å$^{-3}$ | −0.884 | −0.889 |

**Table 2**  Selected bond lengths [Å] and angles [°] for $[Ru^{II}(terpy)(bipy)Cl]Cl\cdot2H_2O$ and $[Ru^{II}(terpy)(en)Cl]Cl\cdot3H_2O$

| $[Ru^{II}(terpy)(bipy)Cl]Cl\cdot2H_2O$ | | | | $[Ru^{II}(terpy)(en)Cl]Cl\cdot3H_2O$ | |
|---|---|---|---|---|---|
| MOL1 | | MOL2 | | | |
| **Bond lengths [Å]** | | | | | |
| Ru1–N1 | 2.079(10) | Ru1–N31 | 2.063(11) | Ru1–N1 | 2.06(3) |
| Ru1–N12 | 1.943(10) | Ru1–N42 | 1.961(10) | Ru1–N12 | 1.93(3) |
| Ru1–N18 | 2.070(11) | Ru1–N48 | 2.069(11) | Ru1–N18 | 2.05(3) |
| Ru1–N19 | 2.041(10) | Ru1–N49 | 2.071(11) | Ru1–N19 | 2.14(3) |
| Ru1–N30 | 2.053(11) | Ru1–N60 | 2.036(10) | Ru1–N22 | 2.10(3) |
| Ru1–Cl1 | 2.413(3) | Ru1–Cl3 | 2.421(4) | Ru1–Cl1 | 2.429(9) |
| **Angle [°]** | | | | | |
| N12–Ru1–N19 | 100.7(4) | N42–Ru2–N60 | 98.7(4) | N12–Ru1–N22 | 95.6(11) |
| N12–Ru1–N30 | 178.6(4) | N42–Ru2–N49 | 175.7(4) | N12–Ru1–N19 | 175.9(11) |
| N19–Ru1–N1 | 89.7(4) | N60–Ru2–N31 | 90.2(4) | N22–Ru1–N1 | 89.5(12) |
| N30–Ru1–N1 | 98.4(4) | N31–Ru2–N49 | 97.3(4) | N19–Ru1–N1 | 101.3(13) |
| N19–Ru1–N18 | 91.9(4) | N60–Ru2–N48 | 91.7(4) | N22–Ru1–N18 | 90.1(12) |
| N30–Ru1–N18 | 102.3(4) | N48–Ru2–N49 | 103.5(4) | N19–Ru1–N18 | 100.0(12) |
| N12–Ru1–N18 | 79.1(5) | N42–Ru2–N48 | 79.9(4) | N12–Ru1–N18 | 79.5(11) |
| N12–Ru1–N1 | 80.2(4) | N42–Ru2–N31 | 79.2(4) | N12–Ru1–N1 | 79.0(12) |
| N19–Ru1–N30 | 79.2(4) | N60–Ru2–N49 | 78.7(4) | N19–Ru1–N22 | 80.3(12) |
| N18–Ru1–N1 | 159.2(4) | N31–Ru2–N48 | 159.1(4) | N18–Ru1–N1 | 158.4(12) |
| N12–Ru1–Cl1 | 86.9(3) | N42–Ru2–Cl3 | 87.1(3) | N12–Ru1–Cl1 | 93.0(8) |
| N19–Ru1–Cl1 | 171.9(3) | N60–Ru2–Cl3 | 174.1(3) | N22–Ru1–Cl1 | 171.3(8) |
| N30–Ru1–Cl1 | 93.3(3) | N31–Ru2–Cl3 | 92.2(3) | N19–Ru1–Cl1 | 91.1(9) |
| N18–Ru1–Cl1 | 86.6(3) | N48–Ru2–Cl3 | 88.0(3) | N18–Ru1–Cl1 | 91.4(8) |
| N1–Ru1–Cl1 | 94.5(3) | N49–Ru2–Cl3 | 95.6(3) | N1–Ru1–Cl1 | 92.3(8) |



**Fig. 1**  Crystal structure of $[Ru^{II}(terpy)(bipy)Cl]Cl\cdot2H_2O$ with the thermal ellipsoids plotted at the 30% probability level. The solvent molecules ($H_2O$) and the second complex cation (MOL2) are omitted for clarity.



**Fig. 2**  Crystal structure of $[Ru^{II}(terpy)(en)Cl]Cl\cdot3H_2O$ with the thermal ellipsoids plotted at the 30% probability level. The solvent molecules ($H_2O$) are omitted for clarity.

and three N atoms of terpy. In $[Ru^{II}(terpy)(en)Cl]Cl\cdot3H_2O$ the deformed octahedral coordination sphere of Ru1 is formed by terpy and en ligands coordinated *via* their N atoms, and the monodentate chloride ligand. Pairs of N and Cl atoms occupy the *trans* positions, N19$_{(bipy)}$ and Cl1 for Ru1 (MOL1) and N60$_{(bipy)}$ and Cl3 for Ru2 (MOL2) in $[Ru^{II}(terpy)(bipy)Cl]Cl\cdot2H_2O$, and N22$_{(en)}$ and Cl1 atoms in $[Ru^{II}(terpy)(en)Cl]Cl\cdot3H_2O$. In both $[Ru^{II}(terpy)(bipy)Cl]Cl\cdot2H_2O$ and $[Ru^{II}(terpy)(en)Cl]Cl\cdot3H_2O$, the tridentate coordination of the terpy causes not only shortening of the Ru–N bond involving the central pyridine ring, when compared to other bonds formed by terpy, but also

significant lowering of the N–Ru–N angle between the coordinate bonds involving the peripheral pyridine rings of terpy, *viz.* N18–Ru1–N1 159.2(4) (MOL1), N31–Ru2–N48 159.0(4)° (MOL2) in $[Ru^{II}(terpy)(bipy)Cl]Cl\cdot2H_2O$ and N18–Ru1–N1 158.4(12)° in $[Ru^{II}(terpy)(en)Cl]Cl\cdot3H_2O$, respectively. No significant difference within the quoted error limits was found for the length of the Ru–Cl bond in both structures.

Analysis of $[Ru^{II}(terpy)(bipy)Cl]Cl\cdot2H_2O$ revealed intra- and intermolecular O–H···O and O–H···Cl bonds involving O atoms of the solvent (see Table 3). Analysis of the crystal packing revealed the presence of intermolecular Ru–Cl···π interactions involving the ring system of terpy of both $[Ru^{II}(terpy)(bipy)Cl]^+$

**Table 3** Hydrogen bonds [Å and °] for [Ru$^{II}$(terpy)(bipy)Cl]Cl·2H$_2$O and [Ru$^{II}$(terpy)(en)Cl]Cl·3H$_2$O

| D–H···A | d(D–H) | d(H···A) | d(D···A) | <(DHA) |
|---|---|---|---|---|
| **[Ru$^{II}$(terpy)(bipy)Cl]Cl·2H$_2$O** | | | | |
| O1–H1A···Cl2 | 0.850 | 1.955 | 2.805 | 178.96 |
| O1–H1B···O2i | 0.884 | 2.472 | 3.226 | 143.49 |
| O2–H2C···O1i | 0.846 | 2.523 | 3.226 | 141.18 |
| O2–H2B···O3 | 0.869 | 2.491 | 2.985 | 116.73 |
| O3–H3B···Cl4ii | 0.870 | 2.415 | 3.232 | 156.49 |
| O3–H3C··· Cl2i | 0.876 | 2.271 | 2.949 | 134.16 |
| O4–H4B···Cl2 | 0.870 | 2.138 | 2.909 | 147.38 |
| O4–H4C···Cl4iii | 0.870 | 2.753 | 3.213 | 114.50 |

Symmetry code: i = −x + 1, −y + 2, −z + 1; ii = −x, −y + 1, −z + 1; iii = −x, −y + 1, −z

| D–H···A | d(D–H) | d(H···A) | d(D···A) | <(DHA) |
|---|---|---|---|---|
| **[Ru$^{II}$(terpy)(en)Cl]Cl·3H$_2$O** | | | | |
| N19–H19A···O3 | 0.900 | 2.412 | 3.138 | 137.89 |
| N22–H22A···Cl2 | 0.900 | 2.460 | 3.238 | 144.88 |
| N22–H22B···Cl1i | 0.900 | 2.433 | 3.307 | 164.06 |
| O1–H1C···O5 | 0.851 | 2.217 | 3.068 | 179.67 |
| O2–H2B···O2ii | 1.005 | 2.567 | 3.458 | 147.74 |
| O2–H2C···O4iii | 0.849 | 2.082 | 2.931 | 179.72 |
| O3–H3B···O5iv | 0.892 | 2.310 | 3.021 | 136.58 |
| O3–H3C···Cl1 | 0.854 | 2.450 | 3.304 | 179.30 |
| O4–H4B···Cl2 | 0.845 | 2.205 | 3.049 | 178.72 |
| O4–H4C···O5v | 0.896 | 2.412 | 3.308 | 177.75 |
| O5–H5B···O3iv | 1.193 | 2.202 | 3.021 | 122.87 |
| O5–H5C···O2iii | 0.917 | 2.300 | 143.15 | 3.082 |

Symmetry code: i = x − 1, y, z; ii = −x, −y, −z + 1; iii = −x − 1, −y − 1, −z; iv = −x − 1, −y − 1, −z − 1; v = x + 1, y, z.

cations, with a Cl1···π[1 + x, 1 + y, z] distance of 3.760(6) Å and a Cl3···π[−1 + x, y, z] distance of 3.675(7) Å. Analysis of the crystal packing in [Ru$^{II}$(terpy)(en)Cl]Cl·3H$_2$O revealed a series of intramolecular interactions involving O atoms of water molecules, N atoms of en or Cl$^-$ ion, and the intermolecular N–H···Cl and O–H···O interactions (see Table 3). Also, intermolecular π···π interactions were detected between the six-membered N1···C6 rings of terpy, with a distance of 3.74(3) Å.

## Structure of [Ru$^{II}$(terpy)(bipy)Cl]Cl and [Ru$^{II}$(terpy)(en)Cl]Cl in solution as determined by NMR spectroscopy

The following NMR measurements were performed to identify the nature of the complexes in solution: $^1$H, $^{13}$C, $^{15}$N, $^1$H–$^{13}$C HSQC, $^1$H–$^{13}$C HMBC and $^1$H–$^{15}$N HMBC. $^1$H–$^{13}$C HSQC/HMBC and $^1$H–$^{15}$N HMBC spectra for both complexes allowed assigning all peaks unambiguously. For further details and NMR spectra see the ESI.† There are in total 19 protons on the ligands that coordinate to the ruthenium center in the bipy complex. The fact that only 14 signals are observed in the $^1$H NMR spectrum of the [Ru$^{II}$(terpy)(bipy)Cl]$^+$ cation is consistent with the $C_s$ symmetry in solution. The Ru, Cl, central nitrogen atom of terpy and both nitrogen atoms of bipy and en are on the mirror plane. Similar symmetry of the terpy ligand and characteristic signal location for the coordinated ethylenediamine were observed for the [Ru$^{II}$(terpy)(en)Cl]$^+$ cation in solution, in agreement with the $C_s$ symmetry of the complex. However, there is a slight inequivalence between the two halves of the terpy ligand in the latter complex. The $^{13}$C NMR spectrum reveals a weak splitting (0.04 ppm) of the C6/C6″ signals, probably due to an asymmetrical contact of the NH$_2$(II) protons from the en ligand and H6/H6″ protons from the terpy ligand. When the NH$_2$(II) protons were saturated in the NOE difference experiment, an enhancement (4.5%) was noticed for H6 and/or H6″ signals, which suggests that such an interaction is possible.

## Spontaneous aquation of [Ru$^{II}$(terpy)(bipy)Cl]$^+$ and [Ru$^{II}$(terpy)(en)Cl]$^+$ in aqueous solution

The [Ru$^{II}$(terpy)(bipy)Cl]$^+$ complex showed a characteristic absorbance maximum at 484 nm which shifted to 474 nm (i.e. a shift of 10 nm) during the aquation reaction in a neutral solution over a period of 7 h at 25 °C, without a significant change in the absorbance intensity (see Fig. 3a). The [Ru$^{II}$(terpy)(en)Cl]$^+$ complex shows characteristic absorbance maxima at 497 and 535 nm which rapidly shift to 483 and 527 nm during the aquation reaction over a period of 7 min at 25 °C (see Fig. 3b).

The spectral changes reported for the [Ru$^{II}$(terpy)(bipy)Cl]$^+$ complex are in agreement with those reported in ref. 2 and 24 (see Table 4), but differ significantly from that reported in ref. 6a. The latter can be ascribed to the use of a PBS buffer that effectively displaced coordinated water during the aquation
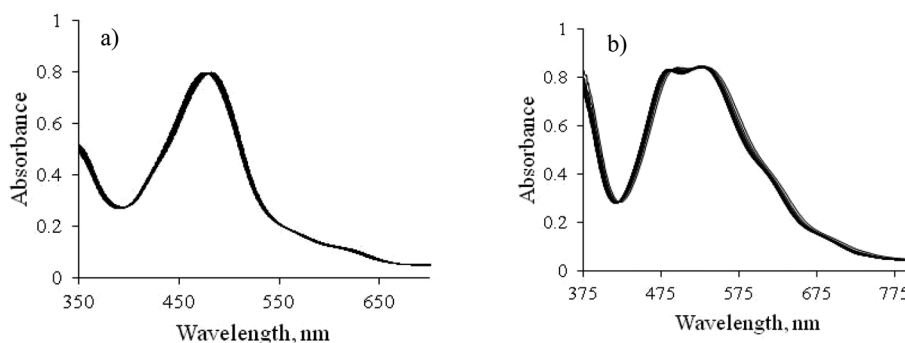


**Fig. 3** Typical UV-Vis spectral changes observed during the spontaneous aquation of [Ru$^{II}$(terpy)(N^N)Cl]$^+$ in the absence of added chloride. Experimental conditions: (a) N^N = bipy, [Ru(II)] = 8.2 × 10$^{-5}$ M and (b) N^N = en, [Ru(II)] = 1.7 × 10$^{-4}$ M; T = 25 °C, I = 0 M, l = 1 cm; spectra recorded every 1000 s (a) and 40 s (b).

**Table 4** Summary of visible spectral data for [Ru(terpy)(N^N)X]$^{2+/+}$ complexes reported in the literature

| X | [Ru$^{II}$(terpy)(bipy)X]$^{2+/+}$ | | [Ru$^{II}$(terpy)(en)X]$^{2+/+}$ | |
|---|---|---|---|---|
| | $\lambda_{max}$, nm ($\varepsilon$, M$^{-1}$ cm$^{-1}$) | Ref. | $\lambda_{max}$, nm ($\varepsilon$, M$^{-1}$ cm$^{-1}$) | Ref. |
| Cl$^-$ | 486 | 24 | 481 (4433), 539 (3524) | 5 |
| | | | 464 (10 000) | 25 |
| H$_2$O | 484 (9800) | This work | 497 (5500), 535 (4400) | This work |
| | 477 (9600) | 2 | 466 (12 000) | 25 |
| | 476 | 24 | | |
| OH$^-$ | 474 (9750) | This work | 483 (4800), 527 (4900) | This work |
| | 508 | 2 | | |
| | 510 (8950) | This work | 530 (4750), 599 (4500) | This work |

reaction of the chlorido complex.[26] In the case of the [Ru$^{II}$(terpy)(en)X]$^{2+/+}$ complexes there are two complications that can account for the observed discrepancies in the spectral data.[5,25] First of all, the [Ru$^{II}$(terpy)(en)Cl]$^+$ complex rapidly aquates (see the following discussion) and a high chloride concentration is required to stabilize the chlorido complex in solution. Secondly, the [Ru$^{II}$(terpy)(en)H$_2$O]$^{2+}$ complex is not stable in aqueous solution over longer periods of time (days and weeks), and its decomposition is accompanied by a shift in the maximum at 483 nm to approx. 470 nm with a significant increase in the intensity of the band.

A first-order fit of the spectral changes reported in Fig. 3a at 460 nm resulted in an observed rate constant of $(1.1 \pm 0.1) \times 10^{-4}$ s$^{-1}$ at 25 °C, which is in close agreement with the value given in ref. 27, viz. $(8–9.7) \times 10^{-5}$ s$^{-1}$, but higher than the one reported in ref. 28, viz. $t_{1/2}$ = 200 min, i.e. $5.8 \times 10^{-5}$ s$^{-1}$. However, this observation contradicts claims in the literature[3,4] that the aquation of [Ru$^{II}$(terpy)(bipy)Cl]$^+$ and related substitution reactions are orders of magnitude faster than those found in the present study. A similar treatment of the spectral data given in Fig. 3b for the [Ru$^{II}$(terpy)(en)Cl]$^+$ complex at 400 nm resulted in an observed rate constant of $(7.0 \pm 0.1) \times 10^{-3}$ s$^{-1}$ at 25 °C, demonstrating that the en complex aquates ca. 64 times faster than the bipy complex.

ESI-MS spectra were recorded for both aqua complexes and are reported in Fig. S1 and S2 (ESI†). In the case of [Ru(terpy)(bipy)(H$_2$O)]$^{2+}$, the signals at 508.07 and 526.04 were assigned to [Ru(terpy)(bipy)(OH)]$^+$ and {[Ru(terpy)(bipy)(OH)]$^+$ + H$_2$O},

respectively (Fig. S1c†). The signal at 259.54 was assigned to [Ru(terpy)(bipy)(N$_2$)]$^{2+}$ (Fig. S1b†) since Ru(II) aqua complexes are generally known to coordinate to dinitrogen, used as the carrier gas during the measurements.[29] In the case of [Ru(terpy)(en)(H$_2$O)]$^{2+}$, the signals at 412.07 and 430.04 were assigned to [Ru(terpy)(en)(OH)]$^+$ and {[Ru(terpy)(en)(OH)]$^+$ + H$_2$O}, respectively (Fig. S2c†). The signal for [Ru(terpy)(en)(N$_2$)]$^{2+}$ (Fig. S2b†) was observed at 211.54. In all cases spectral simulations for the suggested complex species agreed exactly with the experimental data.[30]

The p$K_a$ value of the [Ru$^{II}$(terpy)(bipy)(H$_2$O)]$^{2+}$ complex was determined from a spectrophotometric pH titration during which the band of the aqua complex at 474 nm shifts to that of the hydroxo complex at 510 nm along with a 10% decrease in intensity (see Fig. 4a). Similar spectral changes have been reported in the literature (see Table 4).[2] The p$K_a$ value was found to be $9.83 \pm 0.03$ at 25 °C, which is close to the value of 9.7 reported in ref. 2, but differs significantly from the values of $5.19 \pm 0.06$ at 22 °C and $7.32 \pm 0.02$ reported in ref. 3 and 6a, respectively. At present, we do not have a logical explanation for these apparent discrepancies. For the [Ru$^{II}$(terpy)(en)(H$_2$O)]$^{2+}$ complex the pH titration is shown in Fig. 4b from which a p$K_a$ value of $10.83 \pm 0.03$ at 25 °C was estimated. The p$K_a$ values reported in the literature are summarized in Table 5. Noteworthy is our finding that the p$K_a$ value increases from 9.83 to 10.43 for the bipy complex and from 10.83 to 11.35 for the en complex on increasing the ionic strength from zero to 1.0 M. This trend can be accounted for by the reverse protonation reaction between [Ru$^{II}$(terpy)(N^N)(OH)]$^+$ and H$^+_{aq}$, for which the rate constant is expected to increase with increasing ionic strength, such that $K_a$ will decrease and p$K_a$ will increase. Furthermore, the approximately one unit higher p$K_a$ value for the en complex suggests that the coordinated water molecule is bound more weakly to the Ru(II) center than for the bipy complex (see further discussion), which is in good agreement with the lability of the corresponding chlorido complexes reported above. All in all, these p$K_a$ values are very reasonable for polypyridyl Ru(II) aqua complexes.

### Reactions of [Ru$^{II}$(terpy)(N^N)(H$_2$O)]$^{2+}$ with chloride

On the addition of excess chloride to [Ru$^{II}$(terpy)(N^N)(H$_2$O)]$^{2+}$, where N^N = bipy and en, the spectral changes observed are
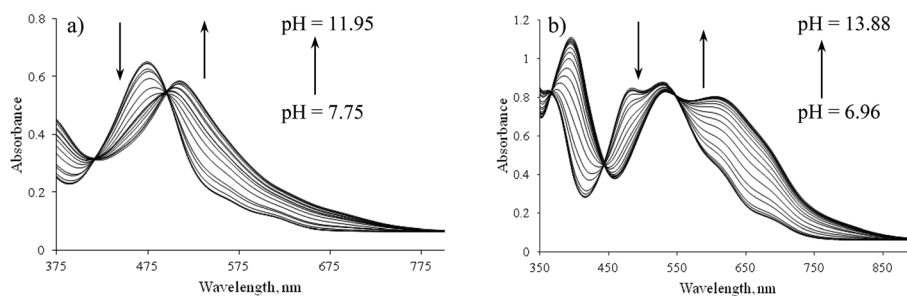


**Fig. 4** Spectra of [Ru$^{II}$(terpy)(N^N)(H$_2$O)]$^{2+}$ recorded as a function of pH in aqueous medium. Experimental conditions: (a) N^N = bipy, [Ru(II)] = $7 \times 10^{-5}$ M and (b) N^N = en, [Ru(II)] = $1.8 \times 10^{-4}$ M (b); T = 25 °C, I = 1.0 M (NaNO$_3$), l = 1 cm.

**Table 5** Summary of $pK_a$ values for $[Ru(terpy)(N^\wedge N)(H_2O)]^{2+}$ reported in the literature[a]

| Medium | $I$, M | $[Ru^{II}(terpy)(bipy)(H_2O)]^{2+}$ | Ref. | $[Ru^{II}(terpy)(en)(H_2O)]^{2+}$ | Ref. |
|---|---|---|---|---|---|
| Water | n.a. | 4.27 and 10.11 | 4 | 9.1[b] | 25 |
| $D_2O$ | n.a. | 5.19 ± 0.06[c] | 3 | | |
| Water | n.a. | 7.32 ± 0.02 | 6a | | |
| Water | ~0 | 9.83 ± 0.03 | This work | 10.83 ± 0.03 | This work |
| NaClO$_4$ | 0.02 | 9.97 ± 0.04 | This work | | |
| NaNO$_3$ | 0.02 | 9.98 ± 0.04 | This work | | |
| Na$_2$HPO$_4$, Na$_3$PO$_4$ | 0.1 | 9.7[d] | 2 | | |
| NaClO$_4$ | 0.1 | 10.16 ± 0.05 | This work | 11.12 ± 0.02 | This work |
| NaNO$_3$ | 0.1 | 10.22 ± 0.05 | This work | 11.11 ± 0.02 | This work |
| NaNO$_3$ | 1.0 | 10.43 ± 0.03 | This work | 11.35 ± 0.01 | This work |

[a] 25 °C. [b] Unknown temperature. [c] 22 °C. [d] 23 °C.

characteristic of the reformation of the chlorido complex, *i.e.* exactly the reverse of that reported in Fig. 3 (see Fig. 5). The absorbance–time traces show clean first-order kinetics (see insets in Fig. 5). The observed rate constants vary linearly with the chloride concentration as shown in Fig. 6. The intercept of the plot is ascribed to the reverse aquation reaction as formulated in reaction (1). The rate law for the reversible aquation of $[Ru^{II}(terpy)(N^\wedge N)Cl]^+$ based on reaction (1) is given by eqn (2), for which $k_1 = (1.7 \pm 0.1) \times 10^{-3}$ s$^{-1}$ and $k_{-1} = (4.3 \pm 0.1) \times 10^{-3}$ M$^{-1}$ s$^{-1}$ at 49.3 °C (bipy complex), $k_1 = (7.9 \pm 0.6) \times 10^{-3}$ s$^{-1}$ and $k_{-1} = (1.28 \pm 0.04) \times 10^{-2}$ M$^{-1}$ s$^{-1}$ at 25 °C (en complex), based on the plots reported in Fig. 6. From these data the equilibrium constants for the aquation reactions are $K_1 = k_1/k_{-1} = 0.40 \pm 0.03$ M at 49.3 °C (bipy complex) and $0.62 \pm 0.07$ M at 25 °C (en complex). It follows that independent of the temperature difference, the en complex is significantly more labile than the bipy complex in both the directions of reaction (1), thus leading to almost the same value for $K_1$. A direct measurement of $k_1$ for the bipy complex at 460 nm, by rapidly dissolving the chlorido complex in pre-heated water under the same experimental conditions, gave a value of $(1.5 \pm 0.2) \times 10^{-3}$ s$^{-1}$, which is indeed close to the intercept found in Fig. 6. An analogous experiment performed for the en complex at 400 nm gave $k_1 = (8.2 \pm 0.2) \times 10^{-3}$ s$^{-1}$, which is also close to the intercept found in Fig. 6.

$$[Ru^{II}(terpy)(N^\wedge N)Cl]^+ + H_2O \underset{k_{-1}}{\overset{k_1}{\rightleftharpoons}} [Ru^{II}(terpy)(N^\wedge N)(H_2O)]^{2+} + Cl^- \tag{1}$$
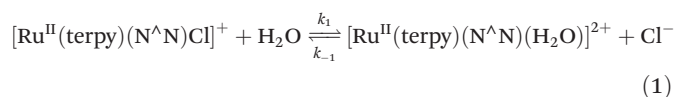
$$k_{obs} = k_1 + k_{-1}[Cl^-] \tag{2}$$

The values of $K_1$ are such that in water as the solvent with a concentration of 55.5 M, a high concentration of chloride is required to prevent the spontaneous aquation reaction. Our findings contradict other reports in the literature,[3,6a] since the authors claim that aquation can be prevented by using 20 or 100 mM chloride, respectively. In this study we found that a chloride concentration higher than 2.5 M is required to completely prevent the aquation of both $[Ru^{II}(terpy)(bipy)Cl]^+$ and $[Ru^{II}(terpy)(en)Cl]^+$. Typical spectral data obtained for the aquation reactions at different added chloride concentrations are summarized in Table 6, from which it follows that the aquation reactions go to completion at 20 and 100 mM chloride, and reach an equilibrium mixture of the aqua and chlorido complexes at 500 mM to 2 M chloride. In 4 M NaCl, no evidence of any aquation reactions was observed. The observed spontaneous aquation of the chlorido complex even in the presence of a large excess of chloride has consequences for any bio-related application. This should be taken into account in the interpretation of kinetic data
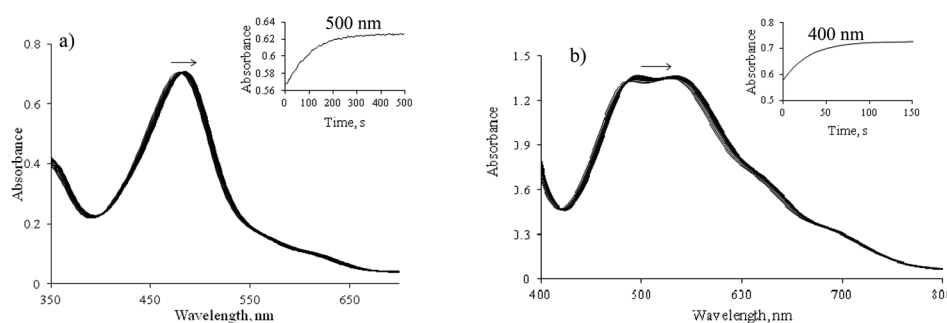


**Fig. 5** Spectral changes recorded for the anation of $[Ru^{II}(terpy)(N^\wedge N)(H_2O)]^{2+}$ by chloride. Experimental conditions: (a) N^N = bipy, $[Ru(II)] = 7.1 \times 10^{-5}$ M, $[Cl^-] = 1.5$ M, $T = 49.3$ °C and (b) N^N = en, $[Ru(II)] = 2.5 \times 10^{-4}$ M, $[Cl^-] = 2$ M, $T = 25$ °C; $I = 2.5$ M (Na$^+$, Cl$^-$, NO$_3^-$), $l = 1$ cm; spectra were scanned every 16 s (a) and 7.5 s (b).

$k_{obs} = (1.7 \pm 0.1) \times 10^{-3} + (4.3 \pm 0.1) \times 10^{-3}$ [Cl⁻]

$K_1 = k_1/k_{-1} = 0.40 \pm 0.03$ M

$k_{obs} = (7.9 \pm 0.6) \times 10^{-3} + (1.28 \pm 0.04) \times 10^{-2}$ [Cl⁻]

$K_1 = k_1/k_{-1} = 0.62 \pm 0.07$ M
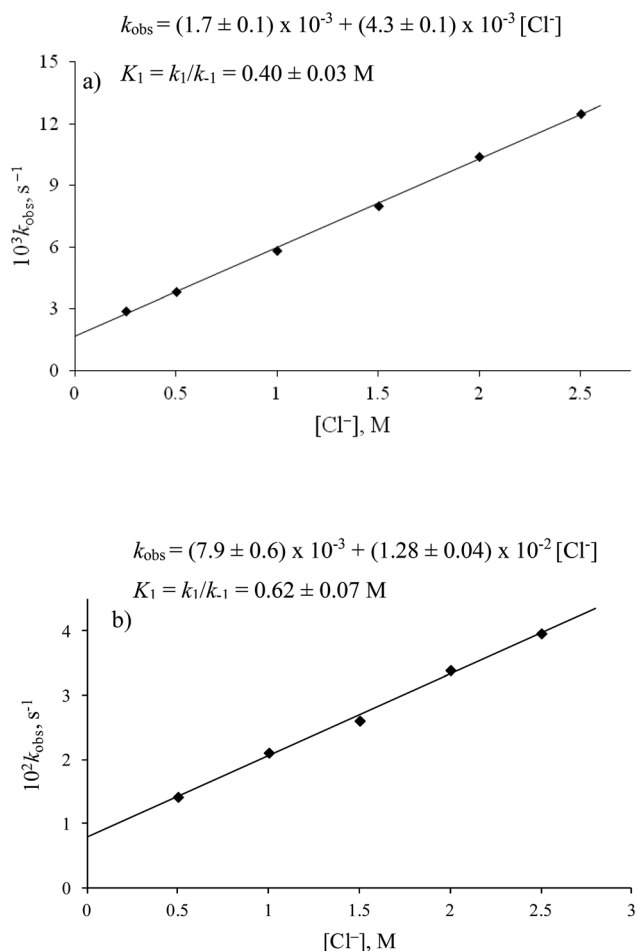
**Fig. 6** Dependence of $k_{obs}$ on [Cl⁻] for the anation of [Ru(terpy)(N^N)(H₂O)]²⁺ by chloride. Experimental conditions: (a) N^N = bipy, [Ru(II)] = $7.1 \times 10^{-5}$ M, $T$ = 49.3 °C and (b) N^N = en, [Ru(II)] = $2.5 \times 10^{-4}$ M, $T$ = 25 °C; $I$ = 2.5 M (Na⁺, NO₃⁻, Cl⁻).

reported in the literature, since aqua complexes are, in general, orders of magnitude more labile than the corresponding chlorido complexes, such that even a small fraction of the aqua complex present in solution can represent the major reaction pathway.

The temperature dependence of reaction (1) for the bipy complex was studied at a chloride concentration of 2.5 M, where the contribution of the reverse aquation reaction (intercept in Fig. 6a) is very small and eqn (2) simplifies to $k_{obs} \approx$ $k_1$[Cl⁻]. The results are summarized in Table S1 (ESI†) and the calculated activation parameters from an Eyring plot are $\Delta H^{\ddagger}$ = 78 ± 2 kJ mol⁻¹ and $\Delta S^{\ddagger}$ = −46 ± 5 J K⁻¹ mol⁻¹. The entropy of activation is in line with an associative interchange ($I_a$) mechanism for the displacement of coordinated water by chloride in reaction (1).

### Reactions of [Ru$^{II}$(terpy)(N^N)(H₂O)]²⁺ with thiourea

Thiourea (TU), being a much stronger nucleophile than chloride, was selected to study the substitution behavior of [Ru$^{II}$(terpy)(N^N)(H₂O)]²⁺, where N^N = bipy and en, in more detail, since it is a neutral entering nucleophile which, in the absence of solvational changes, will simplify the mechanistic interpretation of temperature and pressure activation parameters.

The observed spectral changes for reaction (3) are reported in Fig. 7 and show good first-order behavior as seen from the kinetic trace included as an inset. The values of $k_{obs}$ vary linearly with the thiourea concentration as shown in Fig. S3 and S4 (ESI†), from which it follows that $k_{obs} = k_2$[TU], where $k_2 = (2.08 \pm 0.01) \times 10^{-3}$ M⁻¹ s⁻¹ at 36.3 °C (bipy complex) and $k_2 = (3.74 \pm 0.04) \times 10^{-2}$ M⁻¹ s⁻¹ at 25 °C (en complex). The kinetic data once again demonstrate the significantly higher lability of the en complex even with the 10 °C difference in temperature.

$$[Ru^{II}(terpy)(N^N)(H_2O)]^{2+} + TU \xrightarrow{k_2} [Ru^{II}(terpy)(N^N)TU]^{2+} + H_2O$$

(3)
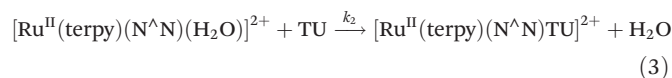
The temperature dependence of reaction (3) was studied at a fixed thiourea concentration of 0.3 (bipy complex) and 0.2 M (en complex) based on the linear concentration dependences reported in Fig. S3 and S4.† The results are presented in Tables S2 and S3 (ESI†), from which it follows that $\Delta H^{\ddagger}$ = 82.9 ± 0.8 kJ mol⁻¹ and $\Delta S^{\ddagger}$ = −29 ± 2 J K⁻¹ mol⁻¹ for the bipy complex and $\Delta H^{\ddagger}$ = 65 ± 2 kJ mol⁻¹ and $\Delta S^{\ddagger}$ = −55 ± 6 J K⁻¹ mol⁻¹ for the en complex. In addition, the effect of pressure was studied under the same conditions and the results are reported in Fig. 8. The volumes of activation ($\Delta V^{\ddagger}$) for the reactions were calculated from the slope (= $-\Delta V^{\ddagger}/RT$) of the plots in Fig. 8 and were equal to −10 ± 1 and −3.8 ± 0.5 cm³ mol⁻¹ for the bipy and en complexes, respectively. The significantly negative values found for both the entropies and volumes of activation support the operation of an associative ligand substitution mechanism, most probably of the associative interchange ($I_a$) type typical for substitution reactions of Ru(II) complexes.[13,14]

**Table 6** Summary of spectral changes observed as a result of aquation of [Ru(terpy)(N^N)Cl]⁺ at different chloride concentrations at 25 °C

| [Cl⁻], M | 0[a] | 0.02[a] | 0.1[a] | 0.5[a] | 1[a] | 1.5[a] | 2[a] | 3 | 4 |
|---|---|---|---|---|---|---|---|---|---|
| [Ru$^{II}$(terpy)(bipy)Cl]⁺ $\lambda$, nm | 474.0 | 474.5 | 476.4 | 479.9[b] | 481.3[b] | 482.4[b] | 482.4[b] | 483.4 | 483.5 |
| [Ru$^{II}$(terpy)(en)Cl]⁺ $\lambda$, nm | 483.1 | — | — | 493.5[b] | 495.8[b] | 496.7[b] | 496.8[b] | 497.2 | 497.2 |
| | 526.8 | — | — | 529.2[b] | 531.4[b] | 533.6[b] | 534.2[b] | 535.0 | 535.0 |

[a] $I$ = 2.5 M (Na⁺, NO₃⁻, Cl⁻). [b] Broad absorption bands due to a mixture of [Ru(terpy)(N^N)Cl]⁺ and [Ru(terpy)(N^N)(H₂O)]²⁺ in solution.
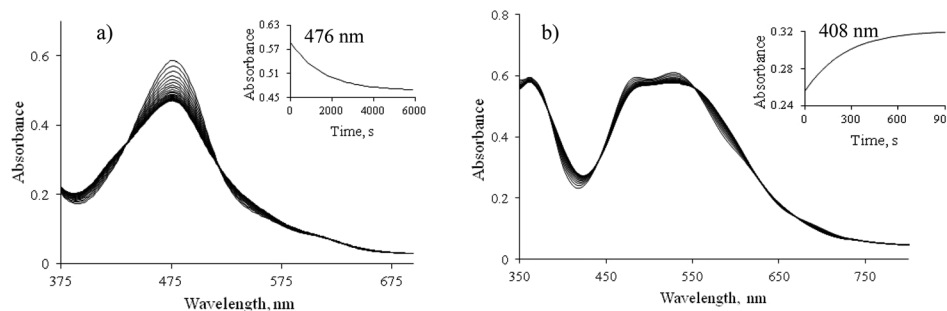
**Fig. 7** Spectral changes observed for the reaction of [Ru$^{II}$(terpy)(N^N)(H$_2$O)]$^{2+}$ with thiourea. Experimental conditions: (a) N^N = bipy, [Ru(II)] = 5.9 × 10$^{-5}$ M, [TU] = 0.3 M, T = 36.3 °C K; (b) N^N = en, [Ru(II)] = 1.2 × 10$^{-4}$ M, [TU] = 0.1 M, T = 25 °C; I = 0.1 M (NaNO₃), l = 1 cm; spectra scanned every 240 s (a) and 50 s (b).
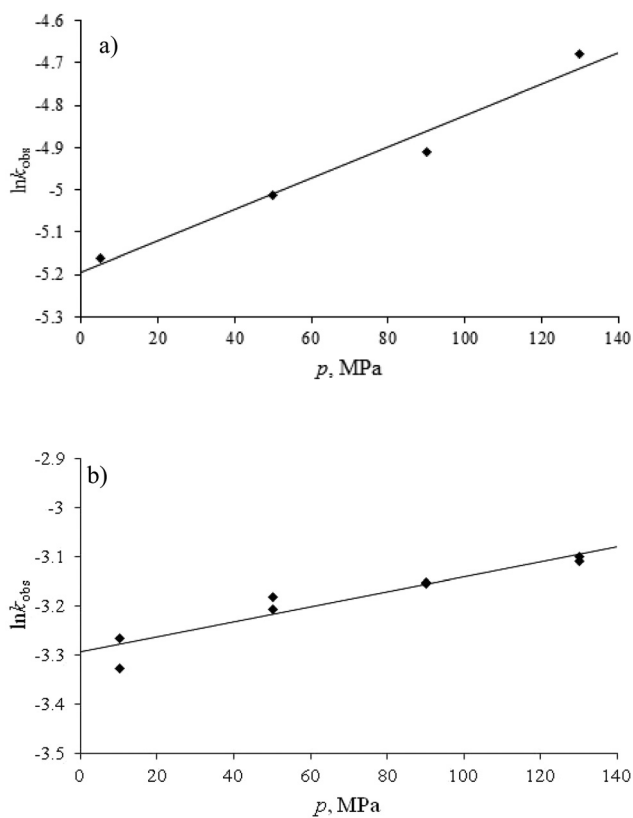


**Fig. 8** Plot of ln $k_{obs}$ versus pressure for the reaction of [Ru$^{II}$(terpy) (N^N)(H$_2$O)]$^{2+}$ with thiourea. Experimental conditions: (a) N^N = bipy, [Ru(II)] = 6.7 × 10$^{-5}$ M, [TU] = 0.5 M, T = 57.5 °C and (b) N^N = en, [Ru(II)] = 4.1 × 10$^{-4}$ M, [TU] = 0.4 M, T = 34 °C; I = 0.1 M (NaNO₃).

### Reaction of [Ru$^{II}$(terpy)(bipy)Cl]$^+$ with thiourea in the presence of chloride

It was practically impossible to study the reaction of [Ru$^{II}$(terpy) (bipy)Cl]$^+$ with thiourea in a direct way due to the competition with the spontaneous aquation reaction that proceeds at a similar rate. For that reason, we started with an equilibrated solution of [Ru$^{II}$(terpy)(bipy)Cl]$^+$ in the presence of an excess chloride and then added thiourea to the mixture of chlorido and aqua complexes. The observed spectral changes clearly indi-

cated the formation of the thiourea complex [Ru$^{II}$(terpy)(bipy) TU]$^{2+}$ at different chloride and thiourea concentrations, for which a typical example is shown in Fig. 9.

The observed first-order rate constant decreased exponentially on increasing the chloride concentration at a fixed thiourea concentration as shown in Fig. 10. This trend suggests that the chlorido complex reacts much more slowly with thiourea than the aqua complex, since the addition of chloride shifts equilibrium (1) to the side of the chlorido complex.

Since the rate constants for the reaction of the aqua complex with chloride and thiourea are very similar (see the data reported above and the mechanistic discussion presented below), a steady state approximation is required to describe the behavior of the aqua complex for the conditions of the data reported in Fig. 10. On the assumption that the more labile aqua complex is the sole reactive species, the following reaction scheme has to be considered:

$$[Ru^{II}(terpy)(bipy)Cl]^+ + H_2O \underset{k_{-1}}{\overset{k_1}{\rightleftharpoons}} [Ru^{II}(terpy)(bipy)(H_2O)]^{2+} + Cl^-$$
$$+ \ TU \downarrow k_2$$
$$[Ru^{II}(terpy)(bipy)TU]^{2+} + H_2O$$
$$(4)$$
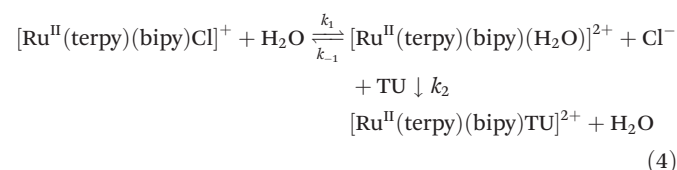
The rate equation for this scheme is $k_{obs} = k_1 k_2 [TU]/$ $\{k_{-1}[Cl^-] + k_2[TU]\}$, which can be linearized to $1/k_{obs} =$ $\{k_{-1}[Cl^-]/k_1 k_2[TU]\} + 1/k_1$. Accordingly, a plot of $1/k_{obs}$ versus $[Cl^-]$ should be linear with an intercept = $1/k_1$ and a slope = $k_{-1}/k_1 k_2[TU]$. Such a plot is presented in Fig. 11 and shows that the suggested mechanism fits well to the experimental data.

From the intercept and slope it follows that $1/k_1 = (8 \pm 1) \times$ $10^2$ s, i.e. $k_1 = (1.2 \pm 0.1) \times 10^{-3}$ s$^{-1}$, and $k_{-1}/k_1 k_2[TU] =$ $(2.4 \pm 0.1) \times 10^3$ s M$^{-1}$ at 49.3 °C. With the values of $k_1$ and $[TU] = 0.1$ M, it follows from the slope that $k_{-1}/k_2 = 0.29 \pm 0.04$, i.e. the reaction with thiourea is approx. 3 times faster than the reaction with chloride, but of the same order of magnitude as assumed above. Using the value for $k_2 = 7.8 \times 10^{-3}$ M$^{-1}$ s$^{-1}$ at 49.3 °C calculated based on the data reported in Table S2,† $k_{-1}$ can be estimated to be $(2.3 \pm 0.3) \times 10^{-3}$ M$^{-1}$ s$^{-1}$, such that $K_1 (= k_1/k_{-1}) = 0.5 \pm 0.1$ M, which is rather close to the value of $0.40 \pm 0.03$ M reported above. We conclude that the analysis of

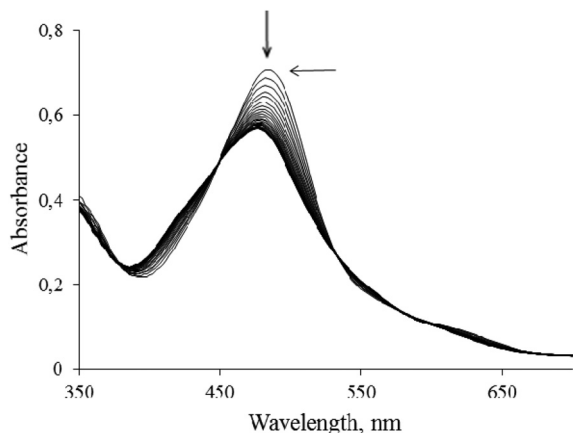**Fig. 9** Spectral changes recorded for the reaction of a [Ru$^{II}$(terpy)(bipy)Cl]$^+$/[Ru$^{II}$(terpy)(bipy)(H$_2$O)]$^{2+}$ mixture with thiourea. Experimental conditions: [Ru(II)] = 7.2 × 10$^{-5}$ M, [Cl$^-$] = 2.5 M, [TU] = 0.5 M, $T$ = 49.3 °C, $l$ = 1 cm; spectra recorded every 60 s.
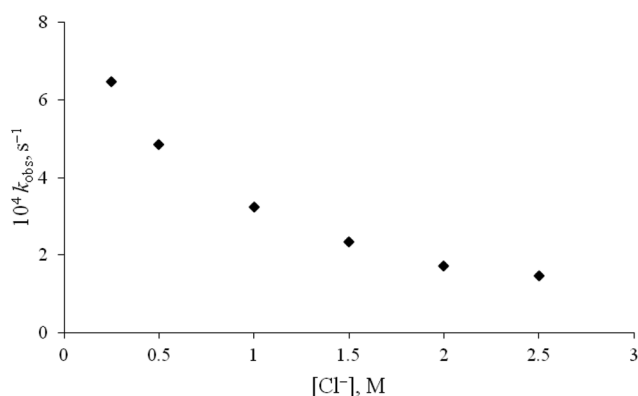


**Fig. 10** Dependence of $k_{obs}$ on [Cl$^-$] for the reaction of a [Ru$^{II}$(terpy)(bipy)Cl]$^+$/[Ru$^{II}$(terpy)(bipy)(H$_2$O)]$^{2+}$ mixture with thiourea. Experimental conditions: [Ru(II)] = 7.2 × 10$^{-5}$ M, [TU] = 0.1 M, $T$ = 49.3 °C, $I$ = 2.5 M (NaNO$_3$).

the kinetic data for the reaction of [Ru$^{II}$(terpy)(bipy)H$_2$O]$^{2+}$ with thiourea in the presence of chloride is very consistent with the remaining data reported here. Furthermore, the data clearly show that the aqua complex is the sole reactive species in solution and reacts orders of magnitude faster than the chlorido complex (see the earlier discussion above). Without any doubt, this will also be the case for the reaction of [Ru$^{II}$(terpy)(en)Cl]$^+$ with thiourea in the presence of chloride.

### Reaction of [Ru$^{II}$(terpy)(en)(H$_2$O)]$^{2+}$ with cyanide

Having studied the reaction with a neutral nucleophile to prevent possible contributions to the activation entropy and activation volume arising from solvational changes, we turned to the reaction with cyanide as a nucleophile which has a similar nucleophilicity but is negatively charged. We studied the reaction of [Ru$^{II}$(terpy)(en)(H$_2$O)]$^{2+}$ with cyanide at pH 10.5, *i.e.* a pH high enough to prevent the protonation of CN$^-$ and low enough to prevent the deprotonation of the coordinated water molecule. The observed spectral changes (Fig. 12) show
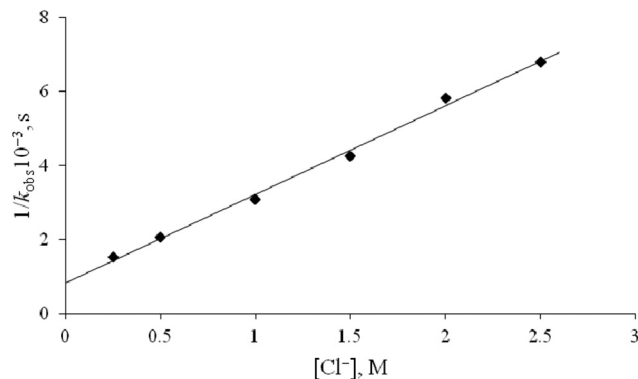


**Fig. 11** Plot of 1/$k_{obs}$ *versus* [Cl$^-$] for the reaction of a [Ru$^{II}$(terpy)(bipy)Cl]$^+$/[Ru$^{II}$(terpy)(bipy)(H$_2$O)]$^{2+}$ mixture with thiourea. Experimental conditions: see Fig. 10.
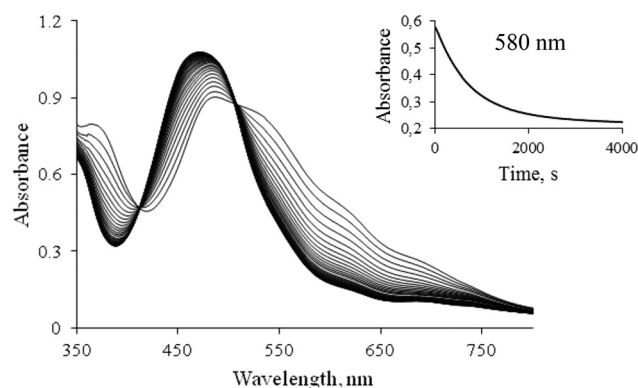


**Fig. 12** Spectral changes recorded for the anation of [Ru$^{II}$(terpy)(en)(H$_2$O)]$^{2+}$ by cyanide. Experimental conditions: [Ru(II)] = 1.9 × 10$^{-4}$ M, [CN$^-$] = 0.05 M, $T$ = 25 °C, $I$ = 1.0 M (NaNO$_3$), pH = 10.5, $l$ = 1 cm; spectra were taken every 120 s.

clean isosbestic points and the kinetic trace in the inset shows perfect pseudo-first-order behavior. The plot of $k_{obs}$ *versus* [CN$^-$] (see Fig. S5, ESI†) shows a linear dependence on the cyanide concentration with a zero intercept of which the slope $k_3$ = (2.91 ± 0.05) × 10$^{-2}$ M$^{-1}$ s$^{-1}$ at 25 °C. A comparison with the data for the reaction with thiourea shows that the rate constants are indeed very similar for these ligands, as expected on the basis of their similar nucleophilicity.

The reaction of [Ru$^{II}$(terpy)(en)(H$_2$O)]$^{2+}$ with CN$^-$ is expected to show a characteristic pH dependence that will be controlled by the p$K_a$ value of the aqua complex, *viz.* 11.25 ± 0.02 at 1 M ionic strength and 25 °C. On increasing the base concentration (pH) the second-order rate constant for the reaction with cyanide slowed down as shown in Fig. 13. At high base concentration the rate constant practically goes to zero, *i.e.* the corresponding hydroxo complex is substitution inert. The data were fitted with a rate law for two parallel reactions of the form $k_3 = (k_{ca} + k_{cb}10^{(14-pK_a)}[OH^-])/(1 + 10^{(14-pK_a)}[OH^-])$, where $k_{ca}$ and $k_{cb}$ represent the rate constants for the reaction of cyanide with the aqua and hydroxo complexes, respectively. A fit of the experimental data to this rate law gave p$K_a$ =
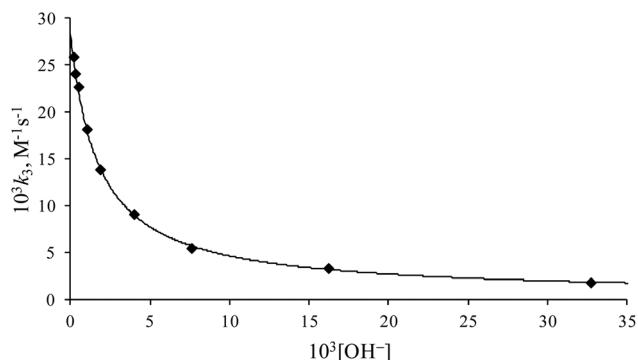
Fig. 13 Plot of $k_3 = k_{obs}/[CN^-]$ versus $OH^-$ concentration for the reaction of $[Ru^{II}(terpy)(en)(H_2O)]^{2+}$ with cyanide. Experimental conditions: $[Ru(II)] = 1.9 \times 10^{-4}$ M, carbonate buffer, $I = 1$ M ($NaNO_3$), $T = 25$ °C.

11.25 ± 0.02, $k_{ca} = (2.84 \pm 0.03) \times 10^{-2}$ $M^{-1}$ $s^{-1}$ and $k_{cb} = (4.4 \pm 2.6) \times 10^{-4}$ $M^{-1}$ $s^{-1}$, suggesting that the aqua complex is approx. 60 times more reactive than the hydroxo complex. In fact, if $k_{cb}$ is taken as zero, the accuracy of the data fit is not affected and results in $pK_a = 11.28 \pm 0.02$ and $k_{ca} = (2.82 \pm 0.03) \times 10^{-2}$ $M^{-1}$ $s^{-1}$. From this, we conclude that the hydroxo complex is indeed substitution inert and all substitution reactions will proceed *via* the significantly more labile aqua complex.

The temperature and pressure dependence of the reaction was studied at pH = 10.5 and the results are summarized in Table S4 (ESI†) and Fig. 14, respectively. The estimated activation parameters are $\Delta H^{\ddagger} = 83 \pm 2$ kJ $mol^{-1}$, $\Delta S^{\ddagger} = +2 \pm 6$ J $K^{-1}$ $mol^{-1}$ and $\Delta V^{\ddagger} = -2 \pm 1$ $cm^3$ $mol^{-1}$. Both the activation entropy and activation volume data are close to zero and, in principle, support the operation of an interchange ($I$) mechanism. However, the significantly more positive values found for these parameters for the reaction with cyanide than for the reaction with thiourea may be due to the fact that cyanide is an anion which will cause charge neutralization coupled with a decrease in solvation and an increase in disorder and partial molar volume in going to the transition state for an inter-
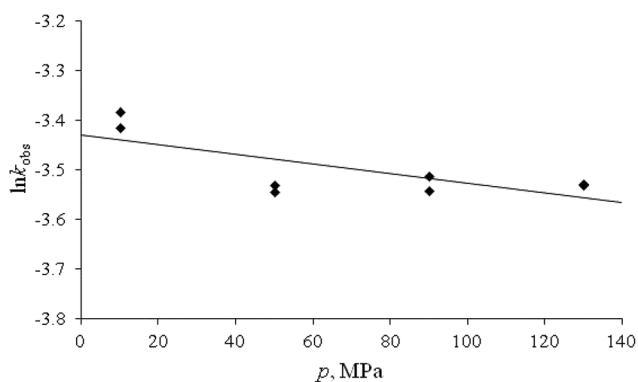


Fig. 14 Plot of $\ln k_{obs}$ versus pressure for the reaction of $[Ru^{II}(terpy)(en)(H_2O)]^{2+}$ with cyanide. Experimental conditions: $[Ru(II)] = 2 \times 10^{-4}$ M, $[CN^-] = 0.2$ M, pH = 10.5 (CAPS buffer), $T = 34$ °C, $I = 1$ M ($NaNO_3$).

change process. Keeping this in mind, the observed activation parameters are still in full agreement with those found for the other reactions studied here, *i.e.* all substitution reactions follow an associative interchange ($I_a$) mechanism.

## Water exchange data for $[Ru^{II}(terpy)(N\wedge N)(H_2O)]^{2+}$

Water exchange reactions were studied for both complexes as a function of temperature using $^{17}O$ NMR techniques under ambient conditions.[31,32] The exchange rates of the water molecules bound to the diamagnetic complexes were obtained from the measurement of line widths of the $^{17}O$ resonance of the water molecule bound to Ru(II) center as a function of temperature. $MnSO_4$ was added as a relaxation agent to allow accurate measurements of the line width of the bound water signal. As a result of very fast water exchange between the bulk and the Mn(II) coordination sphere, as well as due to the long electron relaxation time of the latter ion, the large signal arising from bulk water was successfully suppressed. According to the literature data, the addition of Mn(II) ions has no effect on the measured relaxation rates of the diamagnetic metal complex.[33]

For a water molecule coordinated to a diamagnetic ion, and in the limit of slow exchange,[34] the transverse relaxation rate, $1/T_2^b$, represents the sum of the contributions of the quadrupolar relaxation, $1/T_{2Q}^b$, and of the first-order rate constant for the water exchange, $k_{ex}$ ($k_{ex} = 1/\tau$, where $\tau$ is the mean lifetime of the water molecule in the first coordination sphere of the Ru(II) center), according to eqn (5)

$$1/T_2^b = k_{ex} + 1/T_{2Q}^b \quad (5)$$

The temperature dependence of $k_{ex}$ is given by the Eyring equation (eqn (6)), whereas the quadrupolar relaxation rate was assumed to obey an Arrhenius temperature dependence (eqn (7)), where $(T_{2Q}^b)^{298}$ is the quadrupolar relaxation rate at 298.15 K and $E_Q^b$ represents the corresponding activation energy.

$$k_{ex} = k_B T/h \exp(\Delta S^{\ddagger}/R - \Delta H^{\ddagger}/RT) \quad (6)$$

$$1/T_{2Q}^b = 1/(T_{2Q}^b)^{298} \exp[E_Q^b/R(1/T - 1/298.15)] \quad (7)$$

The values of the experimental transverse relaxation rate, $1/T_2^b$, were calculated according to eqn (8) using the half-width of the $^{17}O$ NMR signal, $\Delta \nu_{1/2}$, measured at each temperature. A typical example of the $^{17}O$ NMR signals observed as a function of temperature is presented for the $[Ru^{II}(terpy)(en)(H_2O)]^{2+}$ complex in Fig. S6 (ESI†).

$$1/T_2^b = \pi \Delta \nu_{1/2} \quad (8)$$

Subsequently, a combination of eqn (5)–(7) was used to fit the experimental values of $1/T_2^b$ and the calculated curves for both the studied complexes are shown in Fig. 15.

The results shown in Fig. 15 clearly demonstrate that the observed relaxation rate, $1/T_2^b$, measured for both Ru(II) complexes, is mainly governed by the quadrupolar relaxation contribution over most of the temperature domain under study. Thus, only a limited number of experiments could be performed at a high temperature where the water exchange
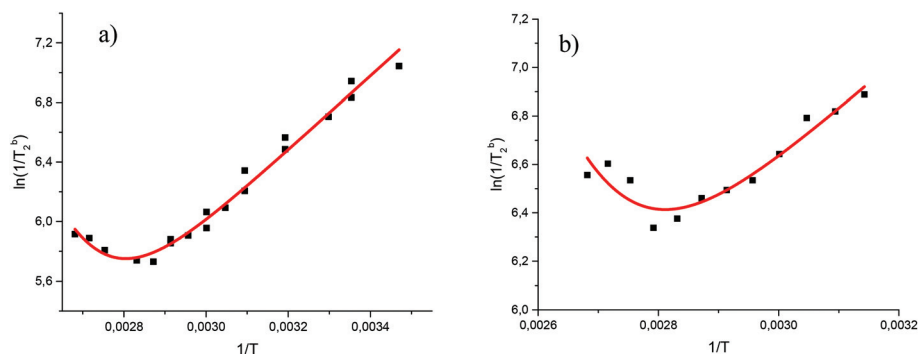
**Fig. 15** Temperature dependence of the relaxation rates, $1/T_2^b$, for the bound-water $^{17}O$ NMR signal of $[Ru^{II}(terpy)(en)(H_2O)]^{2+}$ (a) and $[Ru^{II}(terpy)(bipy)(H_2O)]^{2+}$ (b). Experimental conditions: the concentration of both Ru(II) complexes was 0.03 M in 0.1 M MnSO$_4$ aqueous solution with the addition of 10%-enriched $^{17}OH_2$ to give a total enrichment of 3% $^{17}O$ in the studied samples. See the Experimental section for a detailed description of the sample preparation.

process contributes significantly to the observed line width. Therefore, it was not possible to determine independently the NMR ($(T_{2Q}^b)^{298}$ and $E_Q^b$) and water exchange parameters ($\Delta H^{\ddagger}$ and $\Delta S^{\ddagger}$). In order to obtain a reasonable fit of the experimental data, a two-step fitting procedure was employed. This involved first a fit of the data over the whole temperature range to determine the quadrupolar parameters accurately, followed by a second fit over a narrow temperature range (the selected temperature domain was statistically similar for the kinetic and quadrupolar contributions) using fixed values for $(T_{2Q}^b)^{298}$ and $E_Q^b$ to obtain the activation parameters for the water exchange reactions. The activation parameters were obtained over a small and high temperature range and are subject to large errors, especially the value of $\Delta S^{\ddagger}$. From the estimated activation parameters the water exchange rate constant $k_{ex}$ was calculated and extrapolated to 25 °C. Furthermore, it should be emphasized that the obtained $k_{ex}$ values are subject to large error limits as they result from the difference of two large quantities (see eqn (5)), especially in the case of the $[Ru^{II}(terpy)(bipy)(H_2O)]^{2+}$ complex. Unfortunately, the accuracy of the line width measurements did not allow us to use a high pressure $^{17}O$ NMR probe to measure the activation volume for the water exchange reaction. NMR and water exchange parameters obtained from the above-described fitting procedure are summarized in Table 7. The $E_Q^b$ values determined for both complexes are in the range of known activation energies for the $^{17}O$ quadrupolar relaxation rate of water coordinated to a diamagnetic metal center (viz. 16.6–24.0 kJ mol$^{-1}$).[35] Within

the experimental error limits, the values of $k_{ex}$ are indeed very close for both complexes, but significantly faster than $k_{ex}$ for water exchange on $[Ru(H_2O)_6]^{2+}$, viz. $1.8 \times 10^{-2}$ s$^{-1}$ at 25 °C.[14] Based on the values of $\Delta S^{\ddagger}$ in Table 7, it is concluded that the water exchange process follows a pure interchange ($I$) or weakly associative interchange ($I_a$) mechanism.

### DFT calculations

To obtain more detailed insight into the water exchange mechanism at a molecular level, we performed quantum chemical calculations on the water exchange reactions of $[Ru(terpy)(bipy)(H_2O)]^{2+}$ and $[Ru(terpy)(en)(H_2O)]^{2+}$. We performed the structure optimizations on the well-established and commonly applied level of theory B3LYP/def2svp[36] and obtained, as expected, structures of good quality for the aqua complexes. Comparison of the calculated B3LYP/def2svp structure of $[Ru(terpy)(bipy)(H_2O)]^{2+}$ and the X-ray imaged dication in $[Ru(terpy)(bipy)(H_2O)](PF_6)_2$[37] reveals that the DFT–Ru–N-bond and DFT–Ru–O-bond distances are consequently a bit longer (generally clearly less than 0.1 Å) than in the experimental structure. The same trend can be observed in the study reported by Schramm et al.[36] Inspection of our B3LYP/def2svp-aqua complex structures and the X-ray structures of the corresponding chlorido complexes reported here reveals similar discrepancies in the bond lengths as one would expect on the basis of the $[Ru(terpy)(bipy)(H_2O)]^{2+}$ evaluation.

Subsequently, we studied the water exchange reactions on complexes of the type $[Ru(terpy)(N^\wedge N)(H_2O)]^{2+}$, where N^N = bipy, en and enMe$_2$, and the calculated data are summarized in Table S5 (ESI†). The structures of the ground and transition states for the water exchange reactions $[Ru(terpy)(N^\wedge N)(H_2O)]^{2+}$ + H$_2$O, where N^N = bipy and en, are summarized in Fig. 16.

In the case of the water exchange reaction on the bipy complex (Fig. 16a and b), the entering water molecule in the ground state is located in the second coordination sphere and moves significantly closer to the metal center at a distance of 3.13 Å, which is approximately halfway to the metal center for a bonding distance of 2.18 Å. At the same time the coordinated water molecule in the ground state moves away from the metal

**Table 7** Kinetic and NMR parameters obtained from variable-temperature $^{17}O$ NMR measurements of bound-water transverse relaxation rates for $[Ru^{II}(terpy)(N^\wedge N)(H_2O)]^{2+}$ complexes

|  | $[Ru^{II}(terpy)(en)(H_2O)]^{2+}$ | $[Ru^{II}(terpy)(bipy)(H_2O)]^{2+}$ |
|---|---|---|
| $k_{ex}^{298}$ (s$^{-1}$) | $(8 \pm 2) \times 10^{-1}$ | $(6 \pm 3) \times 10^{-1}$ |
| $\Delta H^{\ddagger}$ (kJ mol$^{-1}$) | $66 \pm 3$ | $69 \pm 5$ |
| $\Delta S^{\ddagger}$ (J K$^{-1}$ mol$^{-1}$) | $-26 \pm 10$ | $-17 \pm 16$ |
| $(T_{2Q}^b)^{298}$ (s$^{-1}$) | $937 \pm 114$ | $1591 \pm 146$ |
| $E_Q^b$ (kJ mol$^{-1}$) | $21 \pm 3$ | $18 \pm 2$ |

a) 0 kcal mol⁻¹

b) +18 kcal mol⁻¹

c) 0 kcal mol⁻¹

d) *0 kcal mol⁻¹*

e) +18 kcal mol⁻¹,*+15 kcal mol⁻¹*

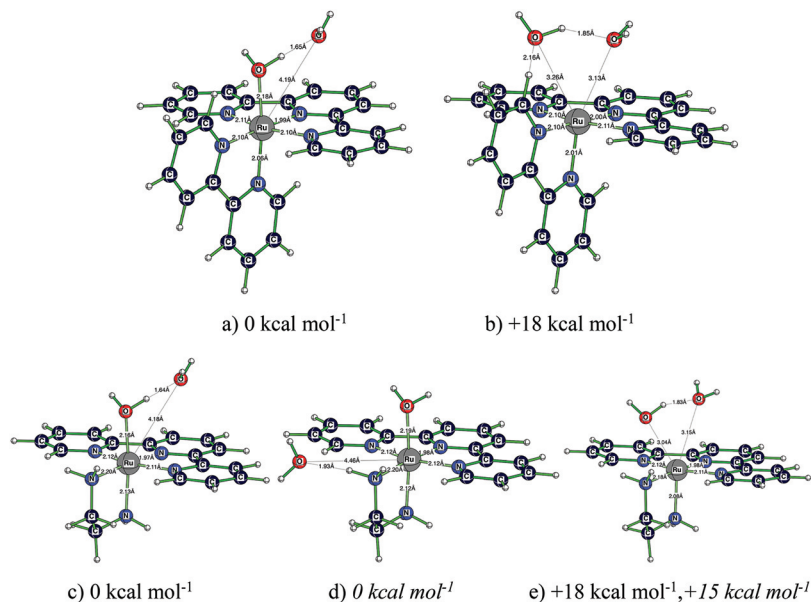**Fig. 16** Calculated (B3LYP/def2svp) ground and transition states for the water exchange reactions $[Ru(terpy)(N^\wedge N)(H_2O)]^{2+}$ + $H_2O$. (a) Ground state for $N^\wedge N$ = bipy; (b) transition state for $N^\wedge N$ = bipy; (c) ground state for $N^\wedge N$ = en with water entering from the top; (d) ground state for $N^\wedge N$ = en with water entering from the side; (e) transition state for $N^\wedge N$ = en. The energy values are related to B3LYP(CPCM)/def2tzvp and ωB97XD(CPCM)/def2tzvp energy calculations on the B3LYP/def2svp structures.

center to a distance of 3.26 Å, such that the transition state is almost symmetrical, typical for a pure interchange (*I*) water exchange mechanism. In the case of the water exchange reaction on the en complex (Fig. 16c–e), the entering water molecule in the ground state can either attach close to the leaving water molecule at a distance of 4.18 Å ($d$(Ru–OH$_2$···OH$_2$) 1.64 Å), similar to that found for the bipy complex, or bind *via* a hydrogen bond to the N–H group of the en ligand at a distance of 1.93 Å ($d$(Ru···OH$_2$) 4.46 Å) (Fig. 16d). This structure is around 3 kcal mol⁻¹ less stable than the structure where the entering water is bound to the leaving one. The calculated hydrogen bond distance in N–H–O is in good agreement with similar values observed experimentally.[37] In the transition state, one water molecule is located at 3.13 Å away from the metal center whereas the other water molecule is even closer to the metal center at a distance of 3.04 Å, presumably due to influences and interactions of the H$_2$N-hydrogen atoms ($d$(NH$_2$·····OH$_2$) 2.46 and 2.62 Å) of the en ligand with this H$_2$O molecule.[37] It follows that in the case of the en complex, the presence of the amine groups seems to assist the water exchange mechanism. The position of the water molecules in Fig. 16e suggests that the transition state has a more compact nature than in the case of the bipy complex, and the mechanism could therefore have a more associative character in terms of an associative interchange ($I_a$) mechanism. The activation barrier for the water exchange reaction starting from the ground state in Fig. 16d for the en complex is *ca.* 3 kcal mol⁻¹ lower than that calculated for the bipy complex (see Table S5†). This could, in principle, account for the significantly faster ligand substitution reactions observed for the en complex as compared to the bipy complex.

In order to check the role of hydrogen bonding during the water exchange reaction of the en complex, calculations were performed for the corresponding complex with enMe$_2$ as a chelate. In this case a very similar behavior to that observed for the bipy complex was found. The activation barrier for this particular ligand is practically the same as that for the bipy complex (see Fig. 17 and Table S5†). Also the bond lengths in the transition state are very close to that reported in Fig. 16b. From this we conclude that hydrogen bonding with the N–H groups can play a significant role in water exchange reactions by lowering the activation barrier by a few kcal mol⁻¹.

**Mechanistic interpretation**

The rate and activation parameters for the ligand substitution reactions studied are summarized in Table 8. The data clearly indicate that very similar rate and activation parameters were found for the reactions of the aqua complexes with chloride, thiourea and cyanide as entering ligands, demonstrating that these complexes show a low nucleophilic discrimination ability. On the other hand, the en complex is *ca.* 30–60 times more labile than the bipy complex for both the aquation and anation reactions studied. The results in Table 8 show a reactivity ratio of the en to the bipy complex of 1 : 64 for the aquation reaction, 1 : 30 for anation by chloride and 1 : 64 for anation by thiourea. This can be accounted for in terms of π back-bonding effects of the bipy chelate as compared to en that will increase the electrophilicity of the Ru(ii) complex and change its electronic nature more in the direction of the less labile Ru(iii) complex. This is also seen in the Ru–Cl bond length (Table 2) which is shorter for the bipy complex than for the en complex. The fact that the en complex is more labile
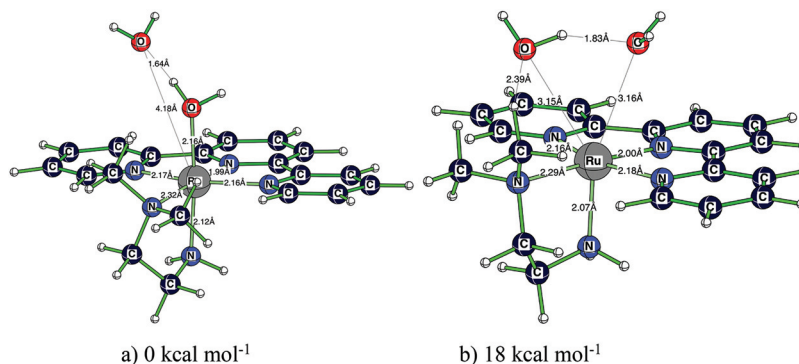
a) 0 kcal mol⁻¹

b) 18 kcal mol⁻¹

**Fig. 17** Calculated (B3LYP/def2svp) ground and transition states for the water exchange reaction $[Ru(terpy)(enMe_2)(H_2O)]^{2+} + H_2O$. (a) Ground state; (b) transition state. The energy values are related to B3LYP(CPCM)/def2tzvp and ωB97XD(CPCM)/def2tzvp energy calculations on the B3LYP/def2svp structures.

**Table 8** Rate constants and activation parameters for the aquation of $[Ru(terpy)(N\wedge N)Cl]^+$ and ligand substitution in $[Ru(terpy)(N\wedge N)(H_2O)]^{2+}$ at 25 °C

| System | $10^3 k_1$, s⁻¹ | $10^3 k_x{}^a$, M⁻¹ s⁻¹ | $\Delta H^{\ddagger}$, kJ mol⁻¹ | $\Delta S^{\ddagger}$, J K⁻¹ mol⁻¹ | $\Delta V^{\ddagger}$, cm³ mol⁻¹ |
|---|---|---|---|---|---|
| $[Ru(terpy)(bipy)Cl]^+ + H_2O$ | $0.11 \pm 0.01^b$ | — | — | — | — |
| $[Ru(terpy)(bipy)(H_2O)]^{2+} + Cl^-$ | | $0.42^{c,f}$ | $78 \pm 2$ | $-46 \pm 5$ | — |
| $[Ru(terpy)(bipy)(H_2O)]^{2+} + TU$ | | $0.58^{d,f}$ | $82.9 \pm 0.8$ | $-29 \pm 2$ | $-10 \pm 1$ |
| $[Ru(terpy)(en)Cl]^+ + H_2O$ | $7.0 \pm 0.1^b$ | — | — | — | — |
| $[Ru(terpy)(en)(H_2O)]^{2+} + Cl^-$ | | $12.8^c$ | — | — | — |
| $[Ru(terpy)(en)(H_2O)]^{2+} + TU$ | | $37^d$ | $65 \pm 2$ | $-55 \pm 6$ | $-3.8 \pm 0.5$ |
| $[Ru(terpy)(en)(H_2O)]^{2+} + CN^-$ | | $29^{e,g}$ | $83 \pm 2$ | $+2 \pm 6$ | $-2 \pm 1$ |

$^a$ $k_x$ denotes $k_{-1}$, $k_2$ or $k_3$ (see the above discussion). $^b$ $I \sim 0$ M. $^c$ $I = 2.5$ M. $^d$ $I = 0.1$ M. $^e$ $I = 1.0$ M. $^f$ Calculated from the activation parameters. $^g$ pH = 10.5.

than the bipy complex for all the studied substitution reactions must be related to its higher Ru(II) character than in the case of the bipy complex. Furthermore, steric hindrance of the bipy ligand as compared to the en chelate could also contribute to this trend. On the other hand, the terpy ligand is also expected to increase the electrophilicity of the Ru(II) center and make it less labile in terms of a $D$ or $I_d$ substitution mechanism, since an increase in electrophilicity will only support an $A$ or $I_a$ mechanism. These tuning effects are of considerable importance in the biomedical application of these complexes since they determine the lability/reactivity of the complexes in solution.

The spontaneous aquation reactions of these complexes are relatively fast. The chlorido complexes aquate fully at room temperature in *ca.* 7 h and *ca.* 7 min for the bipy and en complexes, respectively. At 37 °C these complexes aquate fully in *ca.* 2 h and *ca.* 2 min, respectively. The potential danger of such rapid aquation reactions is the lability of the aqua complexes to interact with potential nucleophiles before they reach their biological targets. The spontaneous aquation reactions can only be suppressed by unrealistically high chloride concentrations between 2 and 4 M. Thus, the 0.1 M chloride concentration in blood is by far not high enough to stabilize the chlorido complex and to prevent the aquation reaction. A serious consequence for any biological application!

The activation parameters reported in Table 8, especially the activation entropy and activation volume data, clearly support an associative interchange ($I_a$) mechanism for the ligand substitution reactions studied. Such an assignment is reasonable in terms of the observed lability of the complexes and the water exchange data reported below. Furthermore, in the case of the substitution of coordinated water by thiourea the observed activation volume is more negative, *i.e.* more associative in the case of the bipy complex, which can be due to the higher electrophilicity expected for the Ru(II) center. Furthermore, the observed activation volume for the substitution of coordinated water by thiourea is more negative, *i.e.* the mechanism has a stronger associative character in the case of the bipy complex, which can be due to the higher electrophilicity expected for the Ru(II) center.

The aqua complexes are characterized by exceptionally high $pK_a$ values indicating a high lability of the coordinated water molecules. The *ca.* 1 $pK_a$ unit higher value for the en complex ($K_a$ is 10 times smaller) demonstrates the weaker binding of water due to the lower electrophilicity of the metal center and a weaker tendency to deprotonate. Under biological conditions these complexes are all present in their aqua form, which are known to be orders of magnitude more labile than the corresponding hydroxo species.

**Table 9** Kinetic parameters for water exchange reactions for some ruthenium(II/III) complexes

| Complex | $k_{ex}{}^a$, s$^{-1}$ | $\Delta H^\ddagger$, kJ mol$^{-1}$ | $\Delta S^\ddagger$, J K$^{-1}$ mol$^{-1}$ | $\Delta V^\ddagger$, cm$^3$ mol$^{-1}$ | Mech. | Ref. |
|---|---|---|---|---|---|---|
| [Ru(terpy)(bipy)(H$_2$O)]$^{2+}$ | $5.7 \times 10^{-1}$ | 69.2 | −17.5 | — | $I/I_a$ | This work |
| [Ru(terpy)(en)(H$_2$O)]$^{2+}$ | $8.2 \times 10^{-1}$ | 65.7 | −26.3 | — | $I/I_a$ | This work |
| [Ru(H$_2$O)$_6$]$^{2+}$ | $1.8 \times 10^{-2}$ | 87.8 | +16.1 | −0.4 | $I$ | 14 |
| [Ru(MeCN)$_6$]$^{2+\,b}$ | $8.9 \times 10^{-11}$ | 140.3 | +33.3 | +0.4 | $I$ | 14 |
| [Ru(H$_2$O)$_6$]$^{3+}$ | $3.5 \times 10^{-6}$ | 89.8 | −48.3 | −8.3 | $I_a$ | 14 |
| [Ru(H$_2$O)$_5$OH]$^{2+}$ | $5.9 \times 10^{-4}$ | 95.8 | +14.9 | +0.9 | $I$ | 14 |

$^a$ 25 °C. $^b$ MeCN exchange.

The rate and activation parameters found for the water exchange reactions of both complexes are summarized along with the relevant literature data in Table 9. In the case of [Ru(MeCN)$_6$]$^{2+}$ the solvent exchange reaction is extremely slow due to the strong Ru–NCMe bond. By way of comparison, water exchange on [Ru(H$_2$O)$_6$]$^{2+}$ is $10^9$ times faster as a result of the much weaker Ru–OH$_2$ bond. In the case of water exchange on the studied [Ru(terpy)(N^N)(H$_2$O)]$^{2+}$ complexes, the line broadening experiments showed that the observed rate constants are, within experimental error, very similar and approximately 50 times faster than that reported for [Ru(H$_2$O)$_6$]$^{2+}$. The N donor chelate effect of the polypyridyl ligands must be responsible for the labilization of the coordinated water molecule, which should show up in the Ru–OH$_2$ bond length and in a higher p$K_a$ value. By way of comparison, the p$K_a$ value for [Ru(terpy)(en)(H$_2$O)]$^{2+}$ is ca. 11 and that of [Ru(H$_2$O)$_6$]$^{2+}$ has been suggested to be between 6 and 8 in the literature.[13,14]

The DFT calculations clearly support the assignment of an $I/I_a$ water exchange mechanism in agreement with earlier assignments made in the literature (see Table 9). In addition, hydrogen-bonding by the amine groups of the ethylenediamine chelate seem to assist the water exchange reaction and can account for the faster ligand substitution reactions found for the en complex. Unfortunately, the $^{17}$O NMR experiments were not accurate enough to show the expected higher lability of coordinated water in the case of the en complex.

## Conclusions and outlook

The results of this study have important implications for the biological application of the studied and closely related complexes as anti-tumor reagents. The fairly rapid aquation reactions of the order of minutes and hours, the extremely high chloride concentrations required to suppress the aquation process, and the much higher lability of the aqua complexes suggest that the studied and closely related complexes will not reach the tumor target when transported via the blood stream, due to the interference of other strong nucleophiles that will bind to the Ru(II) center and suppress the anti-tumor activity observed in cell tests. Therefore, a more specific tuning of the lability of these complexes is required in order to prevent the mentioned complication.

In terms of the relevance of the reported results for processes that control the redox biology of cells involving reactions of Ru$^{II}$-

arene complexes with [NAD$^+$]/[NADH] and formic acid/formate,[8a–c] we suggest that in a similar way, the non-organometallic complexes [Ru$^{II}$(terpy)(N^N)H$_2$O]$^{2+}$, where terpy instead of the arene is now responsible for the labilization of coordinated water, can react with formate to form [Ru$^{II}$(terpy)(N^N)OOCH]$^+$, which in turn reversibly loses CO$_2$ to form [Ru$^{II}$(terpy)(N^N)H]$^+$.[8d] The latter complexes are expected to undergo the same reactions with NAD$^+$/NADH as those suggested for Ru$^{II}$-arene complexes and are presently investigated.

In terms of the relevance of these studies for water oxidation catalysis by single metal site complexes, especially [Ru$^{II}$(terpy)(N^N)H$_2$O]$^{2+}$ and related complexes studied by the groups of Meyer, Berlinguette, Thummel, Masaoka and Sakai,[7] it is noteworthy that the change in N^N chelate is not only accompanied by a change in p$K_a$ value of the coordinated water molecule, but also by a significant change in the ligand substitution rate constants that will control the stability of the catalytic system. Furthermore, in terms of the "water nucleophilic attack (WNA)" or "acid–base" catalytic mechanism suggested in the literature,[7] the nature of the N^N^N and N^N chelates will in turn control the redox potential of the corresponding [Ru$^{II}$–OH$_2$]$^{2+}$, [Ru$^{III}$–OH]$^{2+}$, [Ru$^{IV}$=O]$^{2+}$, [Ru$^V$=O]$^{3+}$, [Ru$^{III}$–OOH]$^{2+}$ and [Ru$^{IV}$–OO]$^{2+}$ species that, in this sequence, form part of the catalytic cycle for the overall reaction 2H$_2$O → 4H$_{aq}{}^+$ + 4e$^-$ + O$_2$. Furthermore, hydrogen bonding networks as found in the present study can affect the lability of such species and play an important role in proton-coupled electron-transfer reactions.[38] Ongoing studies in our laboratories are focused on a systematic variation of the N^N^N and N^N chelates and other donor ligands.

## Author contributions

The manuscript was written through the contributions from all authors. All authors have given approval to the final version of the manuscript.

## Acknowledgements

## References

1 F. P. Dwyer and H. A. Goodwin, *Aust. J. Chem.*, 1963, **16**, 42–50.

2 K. J. Takeuchi, M. S. Thompson, D. W. Pipes and T. Meyer, *J. Inorg. Chem.*, 1984, **23**, 1845–1851.

3 A. Mijatović, B. Šmit, A. Rilak, B. Petrović, D. Čanović and Ž. D. Bugarčić, *Inorg. Chim. Acta*, 2013, **394**, 552–557.

4 A. M. Mijatović, R. M. Jelić, J. Bogojeski, Ž. D. Bugarčić and B. Petrović, *Monatsh. Chem.*, 2013, **144**, 1489–1498.

5 A. Rilak, I. Bratsos, E. Zangrando, J. Kljun, I. Turell, Ž. D. Bugarčić and E. Alessio, *Inorg. Chem.*, 2014, **53**, 6113–6126.

6 (*a*) H. Huang, P. Zhang, Y. Chen, L. Ji and H. Chao, *Dalton Trans.*, 2015, **44**, 15602–15610; (*b*) H. Huang, P. Zhang, Y. Chen, K. Qiu, C. Jin, L. Ji and H. Chao, *Dalton Trans.*, 2016, **45**, 13135–13145.

7 (*a*) J. J. Concepcion, J. W. Jurrs, J. L. Templeton and T. J. Meyer, *J. Am. Chem. Soc.*, 2008, **130**, 16462–16463; (*b*) H.-W. Tseng, R. Zong, J. T. Muckermann and R. P. Thummel, *Inorg. Chem.*, 2008, **47**, 11763–11773; (*c*) S. Masaoka and K. Sakai, *Chem. Lett.*, 2009, **38**, 182–183; (*d*) D. J. Wasylenko, C. Ganesamoorthy, B. D. Koivisto, M. A. Henderson and C. P. Berlinguette, *Inorg. Chem.*, 2010, **49**, 2202–2209; (*e*) D. J. Wasylenko, R. D. Palmer and C. Berlinguette, *Chem. Commun.*, 2013, **49**, 218–227; (*f*) J. D. Blakemore, R. H. Crabtree and G. W. Brudvig, *Chem. Rev.*, 2015, **115**, 12974–13005.

8 (*a*) S. Betanzos-Lara, A. Habtemariam and P. J. Sadler, *J. Mex. Chem. Soc.*, 2013, **57**, 160–168; (*b*) Z. Liu, I. Romero-Canelon, B. Qamar, J. M. Hearn, A. Habtemariam, N. P. E. Barry, A. M. Pizarro, G. J. Clarkson and P. J. Sadler, *Angew. Chem., Int. Ed.*, 2014, **53**, 3941–3951; (*c*) J. J. Soldevilla-Barreda, I. Romero-Canelon, A. Habtemariam and P. J. Sadler, *Nat. Commun.*, 2015, **6**, 6582–6590; (*d*) S. Kern and R. van Eldik, *Inorg. Chem.*, 2012, **51**, 7340–7345.

9 D. Jaganyi, A. Hofmann and R. van Eldik, *Angew. Chem., Int. Ed.*, 2001, **40**, 1680–1683.

10 A. Hofmann, D. Jaganyi, O. Q. Munro, G. Liehr and R. van Eldik, *Inorg. Chem.*, 2003, **42**, 1688–1700.

11 A. Hofmann, L. Dahlenburg and R. van Eldik, *Inorg. Chem.*, 2003, **42**, 6528–6538.

12 B. Petrović, Ž. D. Bugarčić, A. Dees, I. Ivanović-Burmazović, F. W. Heinemann, R. Puchta, S. N. Steimann, C. Corminboeuf and R. van Eldik, *Inorg. Chem.*, 2012, **51**, 1516–1529.

13 P. A. Adcock, F. R. Keene, R. S. Smythe and M. R. Snow, *Inorg. Chem.*, 1984, **23**, 2336–2343.

14 L. Helm and A. E. Merbach, *Chem. Rev.*, 2005, **105**, 1923–1960.

15 B. P. Sullivan, J. M. Calvert and T. Meyer, *J. Inorg. Chem.*, 1980, **19**, 1404–1407.

16 R. van Eldik, W. Gaede, S. Wieland, J. Kraft, M. Spitzer and D. A. Palmer, *Rev. Sci. Instrum.*, 1993, **64**, 1355–1357.

17 *CrysAlis CCD171 and RED171 package of programs*, Oxford Diffraction, 2000.

18 G. M. Sheldrick, *SHELXS97 and SHELXL97*, University of Göttingen, Germany, 1997.

19 M. J. Frisch, G. W. Trucks, H. B. Schlegel, G. E. Scuseria, M. A. Robb, J. R. Cheeseman, G. Scalmani, V. Barone, B. Mennucci, G. A. Petersson, M. Nakatsuji, X. Caricato, H. P. Li, A. F. Hratchian, J. Izmaylov, G. Bloino, J. L. Zheng, H. Sonnenberg, M. Hada, M. Ehara, K. Toyota, R. Fukuda, J. Hasegawa, M. Ishida, T. Nakajima, Y. Honda, O. Kitao, H. Nakai, T. Vreven, J. A. Montgomery, J. E. Peralta Jr., F. Ogliaro, M. Bearpark, J. J. Heyd, E. Brothers, K. N. Kudin, V. N. Staroverov, T. Keith, R. Kobayashi, J. Normand, K. Raghavachari, A. Rendell, J. C. Burant, S. S. Iyengar, J. Tomasi, M. Cossi, N. Rega, J. M. Millam, M. Klene, J. E. Knox, J. B. Cross, V. Bakken, C. Adamo, J. Jaramillo, R. Gomperts, R. E. Stratmann, O. Yazyev, A. J. Austin, R. Cammi, C. Pomelli, J. W. Ochterski, R. L. Martin, K. Morokuma, V. G. Zakrzewski, G. A. Voth, P. Salvador, J. J. Dannenberg, S. Dapprich, A. D. Daniels, O. Farkas, J. B. Foresman, J. V. Ortiz, J. Cioslowski and D. J. Fox, *Gaussian 09, Revision C.01*, Gaussian, Inc., Wallingford CT, 2010.

20 (*a*) A. D. Becke, *J. Phys. Chem.*, 1993, **97**, 5648–5652; (*b*) C. Lee, W. Yang and R. G. Parr, *Phys. Rev. B: Condens. Matter*, 1988, **37**, 785–789; (*c*) P. J. Stephens, F. J. Devlin, C. F. Chabalowski and M. J. Frisch, *J. Phys. Chem.*, 1994, **98**, 11623–11627.

21 F. Weigend and R. Ahlrichs, *Phys. Chem. Chem. Phys.*, 2005, **7**, 3297–3305.

22 J. D. Chai and M. Head-Gordon, *Phys. Chem. Chem. Phys.*, 2008, **10**, 6615–6620.

23 (*a*) V. Barone and M. Cossi, *J. Phys. Chem. A*, 1998, **102**, 1995–2001; (*b*) M. Cossi, N. Rega, G. Scalmani and V. Barone, *J. Comput. Chem.*, 2003, **24**, 669–681.

24 E. Jakubikova, W. Chen, D. M. Dattelbaum, F. N. Rein, R. C. Rocha, R. L. Martin and E. R. Batista, *Inorg. Chem.*, 2009, **48**, 10720–10725.

25 N. Gupta, N. Grover, G. A. Neyhart, P. Singh and H. H. Throp, *Inorg. Chem.*, 1993, **32**, 310–316.

26 Private communication, Prof. Hui Chao, September 2015.

27 D. J. Wasylenko, C. Ganesamoorthy, B. D. Koivisto, M. A. Henderson and C. P. Berlinguette, *Inorg. Chem.*, 2010, **49**, 2202–2209.

28 N. Kaveevivitchai, R. Zong, H.-W. Tseng, R. Chitta and R. P. Thummel, *Inorg. Chem.*, 2012, **51**, 2930–2939.

29 J. Chatt, J. R. Dilworth and R. L. Richards, *Chem. Rev.*, 1978, **78**, 589–625.

30 http://www.sisweb.com/mstools/isotope.htm.

31 J. Maigut, R. Meier, A. Zahl and R. van Eldik, *J. Am. Chem. Soc.*, 2008, **130**, 14556–14569.

32 A. Zahl, P. Igel, M. Weller and R. van Eldik, *Rev. Sci. Instrum.*, 2004, **75**, 3152–3157.

33 L. Helm, L. I. Elding and A. E. Merbach, Water-Exchange Mechanism of Tetraaquapalladium(II), *Helv. Chim. Acta*, 1984, **67**, 1453–1460.

34 A. C. McLaughlin and J. S. Leigh, *J. Magn. Reson.*, 1973, **9**, 296–304.

35 (*a*) J. Berger, M. Kotowski, R. van Eldik, U. Frey, L. Helm and A. E. Merbach, *Inorg. Chem.*, 1989, **28**, 3759–3765; (*b*) Y. Ducommun, K. E. Newmann and A. E. Merbach, *Inorg. Chem.*, 1980, **19**, 3696–3703.

36 F. Schramm, V. Meded, H. Fliegl, K. Fink, O. Fuhr, Z. Qu, W. Klopper, S. Finn, T. E. Keyes and M. Ruben, *Inorg. Chem.*, 2009, **48**, 5677–5684.

37 X.-J. Yang, F. Drepper, B. Wu, W.-H. Sun, W. Haehnel and C. Janiak, *Dalton Trans.*, 2005, 256–267.

38 E. C. Constable, E. L. Dunphy, C. E. Housecroft, M. Neuburger, S. Schaffner, F. Schaper and S. R. Batten, *Dalton Trans.*, 2007, 4323–4332.